Environment International 207 (2026) 110009

Contents lists available at ScienceDirect

Environment International

journal homepage: www.elsevier.com/locate/envint

Full length article

Assessing the severe urban pollution crisis in Sarajevo, Bosnia and Herzegovina: mobile measurements and source characterization

Michael Bauer [a], Jay G. Slowik [a], Marta Via [b], Peeyush Khare [a,e], Benjamin Chazeau [a,f], Kristina Glojek [b,g], Manousos Manousakas [a,h], Zachary C.J. Decker [a,i,j], Asta Gregorič [b,c], Almir Bijedić [d], Enis Krečinić [d], Griša Močnik [b], Katja Džepina [a,b,*], André S.H. Prévôt [a,**]

[a] PSI Center for Energy and Environmental Sciences, 5232 Villigen PSI, Switzerland
[b] University of Nova Gorica, Nova Gorica, 5000, Slovenia
[c] Aerosol d.o.o., Ljubljana 1000, Slovenia
[d] Federal Hydrometeorological Institute of Bosnia and Herzegovina, Sarajevo 71000, Bosnia and Herzegovina
[e] Institute of Climate and Energy Systems (ICE-3): Troposphere, Forschungszentrum Jülich 52428 Jülich, Germany
[f] Aix Marseille Univ., CNRS, LCE, Marseille, France
[g] Institute of Environmental Assessment and Water Research (IDAEA-CSIC), Barcelona 08034, Spain
[h] Environmental Radioactivity & Aerosol Tech. for Atmospheric & Climate Impacts, INRaSTES, National Centre of Scientific Research "Demokritos", Ag. Paraskevi 15310, Greece
[i] Cooperative Institute for Research in Environmental Sciences, University of Colorado Boulder, Boulder, CO 80309, USA
[j] NOAA Chemical Sciences Laboratory, Boulder, CO 80305, USA

ARTICLE INFO

Keywords:
Organic aerosol
Source apportionment
PM1
Mobile measurement
AMS
Sarajevo, Bosnia and Herzegovina
Western Balkans

ABSTRACT

Particulate air pollution is the leading environmental risk factor, contributing substantially to global morbidity and mortality. In the Western Balkans, air quality during winter months is among the poorest observed in Europe. Nevertheless, detailed chemical characterization of air pollution in the region remains limited, although such information is essential for identifying emission sources and supporting effective mitigation strategies. Therefore, a mobile measurement campaign was conducted in Sarajevo (Bosnia and Herzegovina) in January 2023 as part of the SArajevo AEROsol Experiment (SAAERO). The spatial distribution and chemical composition of particle- and gas-phase pollutants were investigated using multiple high-resolution instruments. Organic aerosol (OA), as a key component, accounted for 59% of the total submicron particulate matter (PM_1). Source apportionment of the OA using Positive Matrix Factorization (PMF) resolved five distinct sources: two solid fuel combustion sources (SFC1 and SFC2), traffic (HOA), cooking (COA), and oxygenated OA (OOA). While daytime variation across the city was limited, an east–west pollution gradient emerged during evening hours, largely driven by SFC. SFC contributions to OA ranged from 45 to 54 % in predominantly residential areas outside the city center and amounted to 35 % in the center. In contrast, COA was highest in the center (14%), spatially aligned with restaurant locations.

These findings show that pollution sources contribute non-uniformly in different parts of Sarajevo especially during evening hours. By combining spatially resolved measurements with source apportionment, this study provides valuable insights into pollution sources and their chemical composition in Sarajevo, a highly polluted but still largely understudied area in Europe.

1. Introduction

Atmospheric particulate matter has been shown to be strongly linked with adverse health effects like cardiovascular and respiratory diseases, or cancer leading to increased mortality or shortened life expectancy (Institute for Health Metrics and Evaluation (IHME), 2024a). Fine particulate matter ($PM_{2.5}$) is of special concern, because its small size allows it to penetrate deeply into the respiratory system (Dockery et al., 1993;

* Corresponding author.
** Corresponding author at: PSI Center for Energy and Environmental Sciences, 5232 Villigen PSI, Switzerland.
E-mail addresses: katja.dzepina@psi.ch (K. Džepina), andre.prevot@psi.ch (A.S.H. Prévôt).

https://doi.org/10.1016/j.envint.2025.110009
Received 30 August 2025; Received in revised form 19 November 2025; Accepted 17 December 2025
Available online 19 December 2025

Morawska and Buonanno, 2021; Pope and Dockery, 2006). Most epidemiological studies, however, do not resolve the chemical composition of particles and have focused solely on the total PM mass, assuming equal toxicity for all particles (Cohen et al., 2017; Lelieveld et al., 2015; Weichenthal et al., 2024). In contrast, laboratory studies have demonstrated that different PM components and emission sources exhibit different toxicological effects and that sources driving adverse aerosol health effects are not necessarily the same as those contributing most to PM mass (Cheung et al., 2024; Daellenbach et al., 2020; Park et al., 2018; Wang et al., 2022). Furthermore, aging of PM from various sources can modify and usually enhance their toxicity (Lei et al., 2023; Offer et al., 2022; Tuet et al., 2017). Organic aerosol (OA) and its sources have been identified as important contributors to health risks and are of special interest due to their high contribution to the overall PM mass (Daellenbach et al., 2020; Jimenez et al., 2009). Therefore, understanding the sources driving air pollution is important for the development of more targeted mitigation strategies addressing especially those most detrimental to human health.

While sources have been identified and characterized for various European cities, knowledge is still scarce in Southeast Europe and the Western Balkans in particular (Chen et al., 2022). This is of special concern as it has been frequently shown that air pollution levels there ranks among the worst in Europe based on total PM (Belis et al., 2023; Paradiž et al., 2017). In Bosnia and Herzegovina (BiH), the country of interest in this study, the mortality rate attributed to atmospheric particulate matter pollution is comparable to China and higher than for India (Institute for Health Metrics and Evaluation (IHME), 2024b). The legal framework regarding air quality in BiH is generally aligned with other European countries and follows closely the EU air quality standards. Due to institutional complexity, however, enforcement of the limit values has historically been difficult. Furthermore, several important emission sources such as road traffic and residential sources were unregulated until recently (World Bank, 2024). New regulations and additional strategies have been implemented lately in order to more effectively combat air pollution in the region for the future (Federation of Bosnia and Herzegovina, 2024; CETEOR & E3, 2024). Measurements of air pollution and its composition are an important aspect that help in developing mitigation strategies and monitoring the effectiveness of the chosen measures, especially given the limited financial resources available for funding environmental protection programs and frequent reliance on international funds (CETEOR & E3, 2024). Most available PM measurements in BiH pertain to total mass (Federal Hydrometeorological Institute Bosnia and Herzegovina, 2024; Huremović et al., 2020). Some previous studies have focused on particle-bound metals and polycyclic aromatic hydrocarbons (PAHs), due to their toxic nature (De Pieri et al., 2014; Huremović et al., 2020; Pehnec et al., 2020; Žero et al., 2017,2022), however, for the bulk of PM still only limited information on the chemical composition is available that would be required for a more systematic determination of the sources of pollution. A previous study based on filter measurements during winter investigated different sources and found significant contributions from local sources for all of BiH, specifically from biomass and fossil burning (Grundström et al., 2022).

Sarajevo, the capital of Bosnia and Herzegovina lies in the center of the Western Balkans on the Miljacka River surrounded by mountainous terrain and hills. This geographic location makes the city prone to severe air pollution events, specifically during the winter months. A shallow wintertime boundary layer leads to the accumulation of pollutants, posing substantial health risks to the more than 400.000 inhabitants (Mašić et al., 2019). Since there are no major industrial facilities located within the city of Sarajevo, most of the local pollution is caused by domestic heating and traffic (Grundström et al., 2022; Huremović et al., 2020; Pehnec et al., 2020; Žero et al., 2022). About 90 % of households in BiH are not connected to the central heating grid (Agency for Statistics of Bosnia and Herzegovina, 2015). For the Sarajevo Canton (city and surrounding areas), this share is smaller with 75 % of individual residential buildings using solid fuel as a heating source based on a recent survey for the creation of an emission register. Of these residential buildings the majority used wood (81 % of surveyed households), with coal being another considerable fuel source (13 %), which can significantly impact local air quality. Inefficient and incomplete combustion of wood and/or coal causes high levels of emissions of PAHs, posing significant health risks due to their carcinogenicity (Bruns et al., 2015; Eriksson et al., 2014; Kim et al., 2013).

Traffic is another important source; in 2022, the average age of vehicles in Sarajevo was 19 years with more than 10 % not meeting any of the European emission standards and with more than 60 % classified as Euro 3 or lower (Bosnia and Herzegovina Automobile and Motorcycle Club, 2023). Therefore, traffic likely contributes a great amount to air pollution when compared to western European cities.

Limited information on the pollution composition is available in BiH, even though the overall mortality is 9 %, with Sarajevo specifically a hotspot for pollution (World Bank, 2019). For example, PM concentrations during the winter months frequently exceed 100 μg m^{-3}. The ratio of $PM_{2.5}/PM_{10}$ ranges from 0.5 to 0.6 during the summer months but increases in winter to 0.90–0.99 (Federal Hydrometeorological Institute Bosnia and Herzegovina, 2024) indicating that almost all of the aerosol mass during this time is found as fine particulate matter which is able to penetrate deeper into the lung (Morawska and Buonanno, 2021).

Due to its location, complex geography, and the serious health risks caused by wintertime air pollution, the city of Sarajevo was chosen for the SAAERO (SArajevo AEROsol Experiment) campaign, which took place between August 2022 and March 2023. For a one-month winter period between January–February 2023 an intensive campaign with mobile measurements was carried out to explore the variability of aerosol sources in Sarajevo, the results of which are presented in the following sections. The main advantage of mobile measurements is their ability to obtain spatial information regarding air pollution, thus allowing a detailed exploration of the extent to which various regions of a city are affected. This is of particular interest for locations like Sarajevo, where local emissions are expected to have a large influence and valuable information can be gained on how residents might be affected differently by air pollution depending on the location within the city. Special focus is given to the organic fraction, which often constitutes the majority of the PM_1 mass. The objective was to identify and quantify the most significant sources of OA to allow for the development of more targeted air pollution mitigation strategies to minimize health impacts.

2. Methods

2.1. Measurement campaign and route

The PSI mobile lab measurements in the city of Sarajevo took place from January 12 to February 2, 2023. A map of Sarajevo including the route for mobile measurements is depicted in Fig. 1. Detailed information on the times of mobile measurements, the number of loops driven per day, and the meteorological conditions is presented in Table S1. The loop covers a range of urban environments such as residential, high traffic, and commercially active areas. During the measurement period, mobile measurements were performed on 9 separate days, consisting in total of 39 loops, ranging from 1 to 6 loops per day along the selected route taking around 90 min per loop. This provided a significant amount of data allowing a statistical analysis of the spatial distribution of particle- and gas-phase pollutants. Mobile measurements focused mainly on afternoon and evening periods, when emissions from domestic heating are expected to increase and reach their maximum. When not involved in on-road measurements, the mobile lab was parked at the headquaters of the Federal Hydrometeorological Institute of Bosnia and Herzegovina (FHMZBiH), an urban background site at Sarajevo-Bjelave. There it performed stationary measurements alongside other online and offline instruments for PM chemical composition and concentrations deployed for the SAAERO campaign, which included an Aerosol Chemical

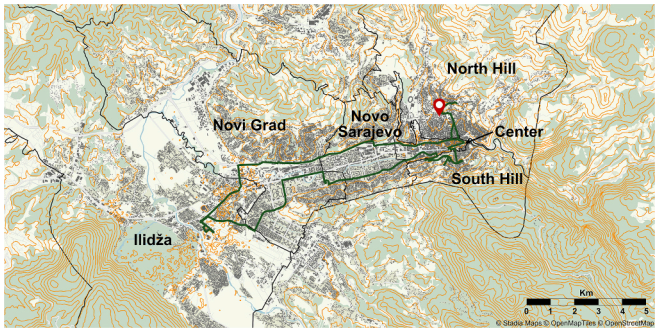

Fig. 1. Measurement Loop in Sarajevo, with the location of the Bjelave site for stationary measurements marked in red. Different regions of Sarajevo are outlined and named in black (see Section 2.5). Yellow contour lines represent elevation at 50 m intervals, highlighting the surrounding hills of Sarajevo. (For interpretation of the references to colour in this figure legend, the reader is referred to the web version of this article.)

Speciation Monitor (Aerodyne Research, Inc., Billerica, MA, USA) (hereafter ACSM) for PM_1 concentration and composition (Ng et al., 2011b) and an Xact 625i Ambient Multi-Metals Monitor (Cooper Environmental Services, OR, USA) for trace metals. Furthermore, long term measurements of PM and some trace gases are routinely carried out by FHMZBiH, providing valuable intercomparison information for instrument QA/QC.

2.2. Mobile laboratory and instrumentation

With the option of high time resolution measurements, mobile laboratories have become an important application for measurements mainly in urban settings to capture spatiotemporal variability in different areas (Coggon et al., 2021; Kolb et al., 2004; Ye et al., 2018; Zhang et al., 2022). The PSI mobile laboratory (IVECO 35S14V Daily) is one of them and has been used and described before for studies in various Europe cities (Bukowiecki et al., 2002; Elser et al., 2018, 2016a; Mohr et al., 2015,2011). For this study, the PSI mobile lab was equipped with state-of-the-art instrumentation for both particle- and gas-phase measurements illustrated in Fig. S1. Two separate inlets for particle- and gas-phase are installed on the roof of the mobile lab, both at a height of 3.2 m and facing towards the rear of the vehicle. While some losses of aerosol particles with larger diameters are expected due to this inlet design, the focus of this work is on submicron particles and gases where such losses are negligible (Ingham et al., 1995; Wen and Ingham, 1995). The particle sampling line consists of stainless-steel tubing, while the sampling line for gas phase instruments is made of polytetrafluoroethylene (PTFE) to minimize wall losses. The particle flow passes through a $PM_{2.5}$ cyclone at 8 L/min. The flow is then reduced to 3 L/min by removing an exhaust flow, passes through a Nafion drier (PermaPure MD-070–12) and is then directed to the instruments. The residence time in the sampling lines is under 2 s. While there is a slight difference between instruments, this does not introduce a detectable time offset in our data, because all measurements were averaged to a 1-minute time resolution to improve signal to noise ratio prior to cross-instrument comparisons (see 2.3. Data Analysis).

This study focuses on non-refractory particle composition (NR-PM_1), in particular on the organic fraction, as measured by an Aerodyne High Resolution Time-of-Flight Aerosol Mass Spectrometer (AMS, Aerodyne Research, Inc., Billerica, MA, USA) (DeCarlo et al., 2006), and equivalent black carbon (eBC) measured by an Aethalometer (Model AE33, Aerosol Magee Scientific, Ljubljana, Slovenia) (Drinovec et al., 2015), respectively. The Aethalometer (hereafter AE33) measurements were converted to eBC using the default MAC, 7.77 m^2g^{-1} at 880 nm, a C_0-value of 1.39 and a harmonization factor of 1.76 as suggested by Müller and Fiebig (2018) (see Supporting Information for a more detailed discussion, about the MAC (Savadkoohi et al., 2024) and C values (Drinovec et al., 2022; Yus-Díez et al., 2025)). Additional gas-phase instrumentation consisted of a Vocus Proton Transfer Reaction Time-of-Flight Mass Spectrometer (TofWerk, Thun, Switzerland) (hereafter Vocus) for measurement of volatile organic compounds (Krechmer et al., 2018) and a Miro MGA-10 (Miro Analytical, Wallisellen, Switzerland) (hereafter Miro) based on mid-infrared laser absorption spectroscopy to simultaneously measure CO(g), CO_2(g), NO(g), NO_2(g), N_2O(g), CH_4(g), SO_2(g), H_2O(g), O_3(g) concentrations (Hundt et al., 2018), where "(g)" denotes gas-phase species throughout this manuscript.

Additional sensors were used to monitor the relative humidity and temperature inside and outside of the vehicle, as well as a GNSS receiver (Navilock NL-8022MP) for acquisition of longitude, latitude, altitude and driving speed. A list of all instrumentation as well as their time resolution at acquisition is presented in Table S2.

2.3. Data analysis

The AMS was operated with a time resolution of 6 sec (3 sec open/3 sec closed) in the mass spectrum (MS) mode. Data from the AMS was post-processed using the data analysis packages "Squirrel" (version 1.66F) and "Pika" (version 1.26F) running in the Igor Pro 9 (Wavemetrics, OR, USA) environment. A constant collection efficiency (CE) of 0.5 was applied to all AMS data. We also considered the composition dependent CE model (CDCE) (Middlebrook et al., 2012). However, the CDCE model is based on the assumption that nitrate and sulphate signals are dominated by ammonium nitrate and sulfuric acid, respectively. In the present study, organic nitrogen and organic sulfur provide a considerable fraction of these signals (Bauer et al., in preparation) and the CDCE cannot be reliably applied. Concentrations from the AMS linearly correlate with various measurements performed at the Sarajevo-Bjelave site when all instruments measured stationary including $PM_{2.5}$ as well as measurements from ACSM and Xact. Certain measurement data had to be retroactively removed due to a loose cable connection leading to intermittent time periods of unreasonably high or low concentrations in the spectrum. During these periods, the mass spectrum showed a clear zig-zag pattern with alternating points being elevated (Fig. S2). By quantifying the absolute difference between adjacent points in baseline regions the affected periods were identified and excluded from further analysis. The remaining data was averaged to 1 min to improve signal to noise ratio, specifically necessary at higher mass to charge ratio (m/z). Standard spectral processing protocols were followed, including m/z calibration, baseline correction and sub-integer peak fitting. High resolution (HR) mass spectral data was exported for Positive Matrix Factorization (PMF) up to a mass to charge ratio (m/z) 120 due to the limited mass resolution of the AMS. Unit mass resolution (UMR) data was included from m/z 121 to 300 in order to utilize information regarding high mass species, specifically regarding PAHs which are known to fragment less (Dzepina et al., 2007). PAH concentrations were also calculated separately according to the method described in Dzepina et al. (2007). Since PAH concentrations in this case are estimated based on signals with $m/z > 200$ to minimize interferences from non-PAH organics, some lighter PAHs are excluded. As a result, absolute PAH-concentrations may be somewhat underestimated. Temporal and spatial trends, however, are expected to remain reliable and provide valuable insight.

Due to unforeseeable circumstances, RIE, RF calibration could not be carried out in the field. Instead, stationary measurements by the ACSM during time periods when the ACSM and AMS obtained data at the same location, were used to calibrate all species of the AMS. This approach was deemed applicable since both instruments consistently showed high correlations and good mass-closure with other on- and offline measurements of PM and its chemical components (Fig. S3). Due to replacement of the AMS servo motor on January 29 which requires physically opening the instrument, separate calibrations were performed for the period before and after this hardware change out of an

abundance of caution.

All other instrument data was also averaged to 1 min time resolution. The Vocus and Miro performed automated background measurements using zero air every 30 min, which were linearly interpolated and subtracted from the ambient measurements. For the AE33, the averaging was performed based on the measured difference in attenuation over 1 min instead of the direct averaging of 1 sec BC data, similar to Hagler et al., 2011. Additionally, the Aethalometer model was used to deconvolve the data into liquid fuel (eBC_{lf}) (mainly traffic related) and solid fuel (eBC_{sf}) (biomass burning and coal combustion) contributions to eBC (Sandradewi et al., 2008). The used Ångström exponents were $\alpha_{lf} = 1.1$ and $\alpha_{sf} = 2.1$ according to Via et al. (in preparation) for this site, which are determined by selecting α_{lf} first from the first percentile of the AAE distribution followed by an iterative approach of minimizing the intercept of the solid fuel fraction of the absorption coefficient b_{abs}^{sf} and m/z 60 from the ACSM (as a biomass burning tracer) (Fuller et al., 2014).

2.4. Positive matrix factorization

Positive Matrix Factorization (PMF) has been frequently used and proven useful for ambient measurements using AMS to determine and distinguish pollution sources for the organic fraction (Chen et al., 2022; Crippa et al., 2014; Lanz et al., 2008; Ulbrich et al., 2009; Zhang et al., 2011). The measurements of OA can be represented as a matrix **X** with a subsequent uncertainty matrix **S**. Each row i of this matrix represents a timepoint, while each column j represents an individual variable (ion or integer m/z). The data matrix **X** can be written as a linear combination in the following form:

$$X = G \cdot F + E \tag{1}$$

Here the two matrices **G** and **F** are an $n \times p$ and $p \times m$ matrix where n and m represent the number of timepoints and variables (ion or integer m/z) and p represents the number of factors the chosen model solution consists of. Therefore, each column in **G** shows the timeseries of a factor while each row of **F** describes the corresponding factor mass spectrum. **E** is the residual matrix, defined by Eq. (1). The **G** and **F** matrices are determined by minimizing the objective function Q, defined as the sum of the squares of the uncertainty-weighted residual matrix (Paatero, 1997; Paatero and Tapper, 1994).

$$Q = \sum_i \sum_j \left(\frac{e_{ij}}{\sigma_{ij}}\right)^2 \tag{2}$$

Here, σ_{ij} are the components of the error matrix **S** representing the measurement precision (Allan et al., 2003). PMF was implemented using the ME-2 engine while configuration of the model as well as post analysis was performed using SoFi (Source Finder, Datalystica Ltd.) (Canonaco et al., 2021, 2013; Paatero, 1999).

The ME-2 solver allows the user to add *a priori* information to the analysis, such as by constraining the profiles and/or timeseries of one or more factors. This is implemented using the a-value approach, shown in Eq. (3) for a hypothetical factor k. The parameter a is a scalar determining the tightness of constraint relative to the anchor and ranges from 0 (fully constrained) to 1 (unconstrained) (Canonaco et al., 2013)

$$f_{kj\_solution} = f_{kj} \pm a \cdot f_{jk} \tag{3a}$$

$$g_{ik\_solution} = g_{ik} \pm a \cdot g_{ik} \tag{3b}$$

To assess the uncertainty of the PMF result due to random errors in data values and modelling errors, bootstrap resampling can be used. For each resampling step, randomly selected rows of the input matrix are replaced or repeated while keeping the dimension the same before performing PMF (Canonaco et al., 2021; Efron, 1979; Paatero et al., 2014). By applying criteria based on expected correlations and profile features the large number of PMF solutions can be evaluated and runs that are environmentally unreasonable e.g., due to rotational ambiguity are rejected.

PMF results were first examined for unconstrained runs ranging from two to ten factors. To assess and in the end confirm the sources of the obtained PMF result, factors were compared to other measurements from the Miro, Vocus, and AE33 in the mobile lab and specific tracers known for certain sources. During mobile measurement periods, large variations and short-term individual point sources may sometimes not be captured entirely by the AMS due to the open-closed cycle, as has been previously observed in mobile measurements (Mohr et al., 2011). Removal of outliers proved to be efficient to compare timeseries more accurately and to avoid the sensitivity of least square estimates to outliers. Therefore, two approaches were used for the comparison: First, a temporal approach (comparison of timeseries) where the top 1 percentile of values was removed. Second, an approach on the spatial scale further described below, which also negates the effect of short pollution spikes and additionally minimizes correlation effects that are due to varying meteorological conditions influencing all parameters simultaneously.

2.5. Spatial averaging of data

Evaluating PMF results and measurement data overall on a spatial scale required some additional averaging of the data. Even in an urban environment, where the driving speed during mobile measurements is not very high, the distance covered during a 1 min period can be large. Therefore, the allocation of a single spatial coordinate to a 1 min datapoint representing this period is insufficient when trying to spatially average the data. Instead, data from the GNSS receiver with a 1 s resolution were used to provide precise location data and the 1 min instrument data were aligned by uniformly assigning the value of each 1 min interval to all the corresponding 1 sec GNSS time points within that minute. The thus "upscaled" mobile measurements were then spatially aggregated using the H3 discrete global grid system (Uber Technologies, Inc., 2025) at resolution 11, meaning that all coordinates falling into a hexagonal cell with an edge length of approximately 25 m are binned together. To ensure statistical relevancy, an additional condition was to use only those hexagonal cells in further evaluations for which datapoints from at least 5 different days were available. Although day-to-day variability on a spatial scale was observed for the measurement data, this study focuses on the averaged spatial distributions to provide a more general overview of how pollution is distributed across the city.

To this end, spatial data was furthermore averaged based on the different municipalities within the Sarajevo canton that our measurement loop crossed (Ilidža, Novi Grad, Novo Sarajevo, Centar, Stari Grad). The two municipalities of Centar and Stari Grad, however, were combined and instead divided by altitude and location south and north of the Miljacka river. This allowed it to further distinguish between areas due to altitude as well as to better capture the differences between the residential areas at higher altitude along the hills, in comparison to the more commercially active area in the city center. The distinction in altitude was set at 560 m which represents the base of the valley, leading to three regions termed North Hill, South Hill, and Center (Fig. 1 and additional information in Fig. S4).

3. Results and discussion

3.1. Overview of measurements

Fig. 2 shows the temporal variation of the PM_1 concentration (NR-PM_1 measured by the AMS and $PM_{2.5}$ eBC concentrations from Aethalometer measurements) with a time resolution of 1 min over the entire campaign. Periods of mobile measurements are highlighted in grey. Gas-phase concentrations for SO_2(g), CO(g) and CO_2(g) measured with the Miro are depicted as well. Mobile measurements carried out on January 14 and January 26–27 in Zenica (BiH) are not part of this work, and the

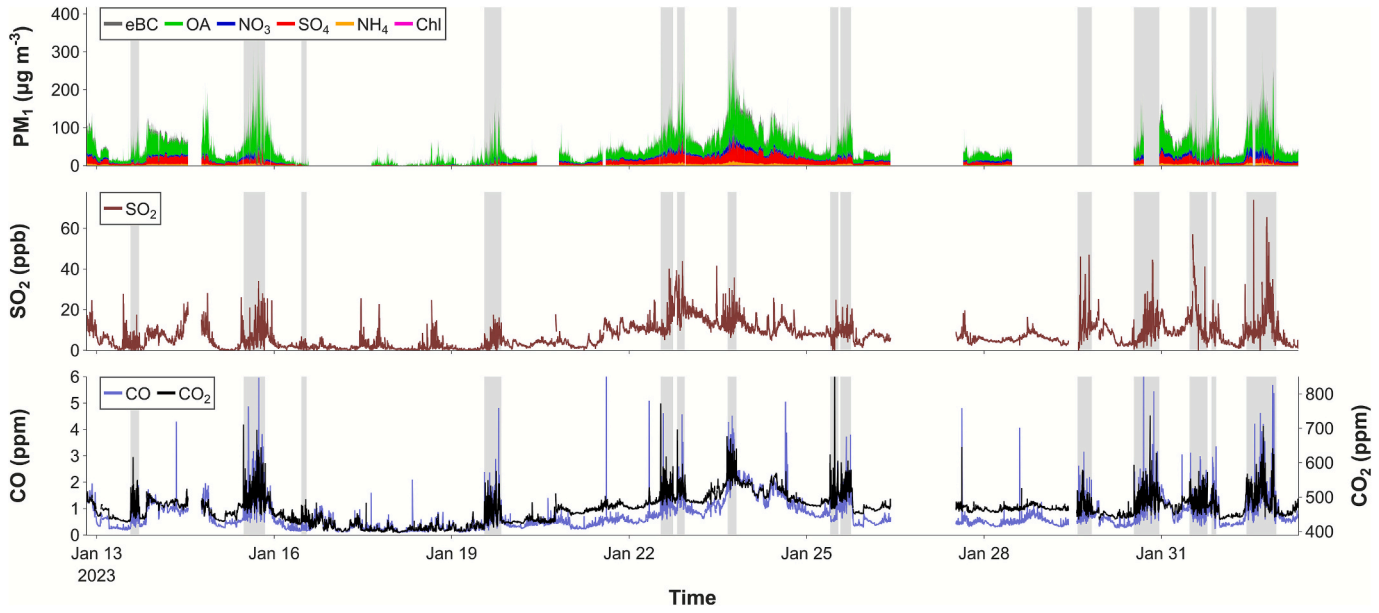

Fig. 2. Temporal evolution of selected particle- and gas-phase components over the entire measurement campaign in Sarajevo. Grey shading indicates periods of mobile measurements.

data therefore not included in Fig. 2. Furthermore, particle concentrations data are unavailable for a period between January, 28–January, 30.

The campaign average PM_1 concentration for stationary and mobile measurements combined was 42.7 µg m^{-3} and 66 % of the total one-minute AMS measurements exceeded the WHO 24-hour $PM_{2.5}$ guideline value of 15 µg m^{-3} (World Health Organization (WHO), 2021). Meteorological conditions, however, induce large variability in the data. Very low concentrations were measured during the period of January 17 to 19 due to precipitation and warmer temperatures (Table S1), while maximum PM_1 concentrations exceeding 100 µg m^{-3} (accounting for 10 % of all data) were observed during periods of pollution accumulation over multiple days due to cold temperatures and a stable planetary boundary layer (PBL). Especially during this period for stationary measurements, concentrations show variation, while the overall composition shows little change. On the other hand, mobile measurement periods showed significant short-duration concentration spikes throughout the campaign due to local emission from point sources reaching a maximum of 396 µg m^{-3}, which are not captured by stationary measurements.

Comparison of the measurement campaign time period with long term PM measurements in Sarajevo show that the average pollution levels were lower compared to other winter periods (European Environment Agency (EEA), 2025). Lower concentrations are mostly due to meteorological conditions involving significant vertical mixing. Throughout the measurement time changes in concentration do not follow a clear diurnal pattern with the average diurnal contributions staying mostly unchanged throughout the day and absolute concentrations increasing proportionally in the afternoons (see Figs. S5 and S6). OA shows the largest contribution to PM_1 with 59 %, followed by particulate sulphate (21 %), nitrate (8 %), eBC (7 %), ammonium (5 %) and very low concentrations of chloride (<0.5 %). The components of the AMS will be termed SO_4, NO_3, NH_4 and Chl throughout this study and their difference between stationary and mobile measurements will be discussed in more detail later.

The middle panel of Fig. 2 shows the time series of SO_2(g) concentrations. While SO_2(g) concentrations have significantly decreased in large parts of Europe in recent decades, pollution levels in BiH remain the highest among European countries (Henschel et al., 2013; Targa et al., 2024), thus contributing to secondary inorganic aerosol formation, as suggested as well from the high SO_4 concentrations, and posing potential adverse health impacts. During this campaign, average SO_2(g) concentrations in Sarajevo were 6.9 ppb of SO_2(g), with peaks of up to 70 ppb observed during mobile measurements, whereas typical European annual SO_2(g) concentrations are below 2 ppb (Targa et al., 2024). The campaign average concentrations for CO_2(g) and CO(g) were 464.8 ppm and 0.7 ppm, respectively, with the highest concentrations again observed during mobile acquisition.

3.2. Source apportionment results

A five-factor solution was determined to best represent the OA data for mobile and stationary measurements as up to 5 factors were fully interpretable and could additionally be confirmed by comparison with external reference profiles, correlations with other tracers measured in the mobile lab, and analysis of the residuals of the PMF run and the values of Q/Q_{exp}. An increase in factors beyond 5 did not result in further improvements in residuals or Q/Q_{exp}. Also, higher order solutions resulted in factors that were not chemically interpretable and showed indications of splitting or mixing of already existing factors (Fig. S7).

Of the resolved factors, traffic-influenced hydrocarbon-like OA (HOA) mainly from traffic, two solid fuel combustion factors (SFC1 and SFC2) related mainly to residential heating, and a cooking-influenced OA (COA) factor are attributed to primary organic aerosol (POA). The fifth factor, oxygenated OA (OOA), is related to aged OA including secondary OA (SOA). While the timeseries of the unconstrained solution appears reasonable and correlate well to external measurements, the factor profiles of COA and SFC2 show high contributions of CO^+, CO_2^+ ions and related components, compared to previously reported factors (Crippa et al., 2014; Elser et al., 2016b; Mohr et al., 2012) indicating some mixing with OOA. To address this, COA and SFC2 were constrained from a solution with a higher number of factors, similar to previous studies (Docherty et al., 2011; Fröhlich et al., 2015). A more detailed explanation of the PMF setup and choice for the PMF solution presented here is provided in the Supporting Information. The factor profiles of the final solution are represented in Fig. 3 with the mass spectra and chemical family composition of the five identified OA factors (Spectra are averaged over 481 bootstrap runs, criteria for the selection of the runs are illustrated in Fig. S9). The factor timeseries are

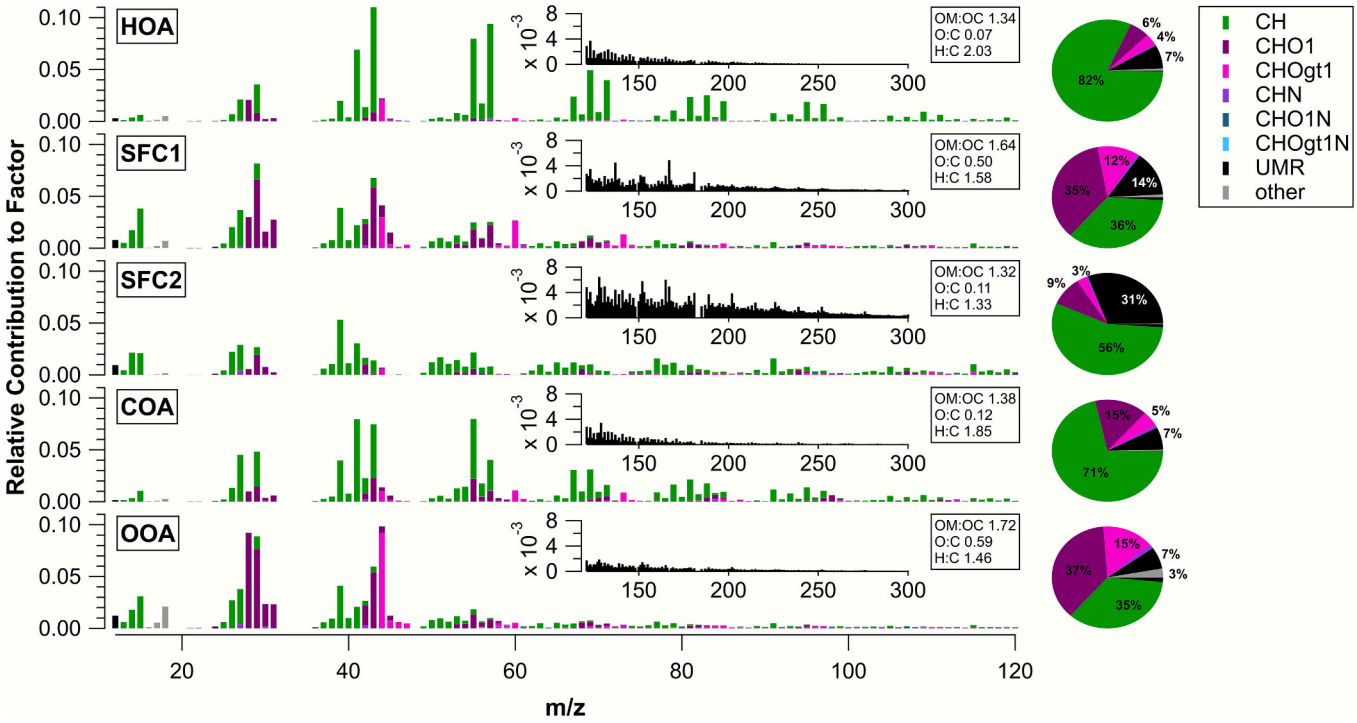

Fig. 3. Mass spectra of the five identified OA factors: HOA, SFC1, SFC2, COA and OOA. Spectra are averaged over 481 bootstrap runs and divided into two regions: One for $m/z < 120$ with individual ions from HR peak fitting and ions colored by their chemical family composition, and a second region in the insets for $m/z > 120$ of UMR masses colored in black.

shown in Fig. 4 together with respective tracers to confirm source attributions. Correlations to those tracers as well as other measurements in Fig. 5 are shown both on a temporal scale (comparison of timeseries) and a spatial scale (comparison of hexagonal cells).

Diurnal patterns of the factor timeseries were used to a lesser extent and with caution since spatial variability during mobile measurements will influence the temporal trends. If considering only stationary measurements, data from the afternoon and evening periods, during which mobile measurements were usually performed, is undersampled, potentially degrading the comparison. Additionally, a meteorological effect on the diurnal distribution is expected due to the location of the measurement station on the hill slope. Diurnals for separated periods of stationary and mobile measurements are shown in Fig. S11.

The HOA profile is mainly composed of the ion series $C_nH^+_{2n+1}$ and $C_nH^+_{2n-1}$, signatures from aliphatic hydrocarbons (Crippa et al., 2013; Ng et al., 2011a), which together contribute more than 80 % to the total factor mass, consistent with primary traffic emissions. The O/C ratio of 0.07 for this factor is in the lower range as the one for HOA in comparative ambient measurements, and comparable to previous mobile measurements (Canagaratna et al., 2015; Crippa et al., 2014; Mohr

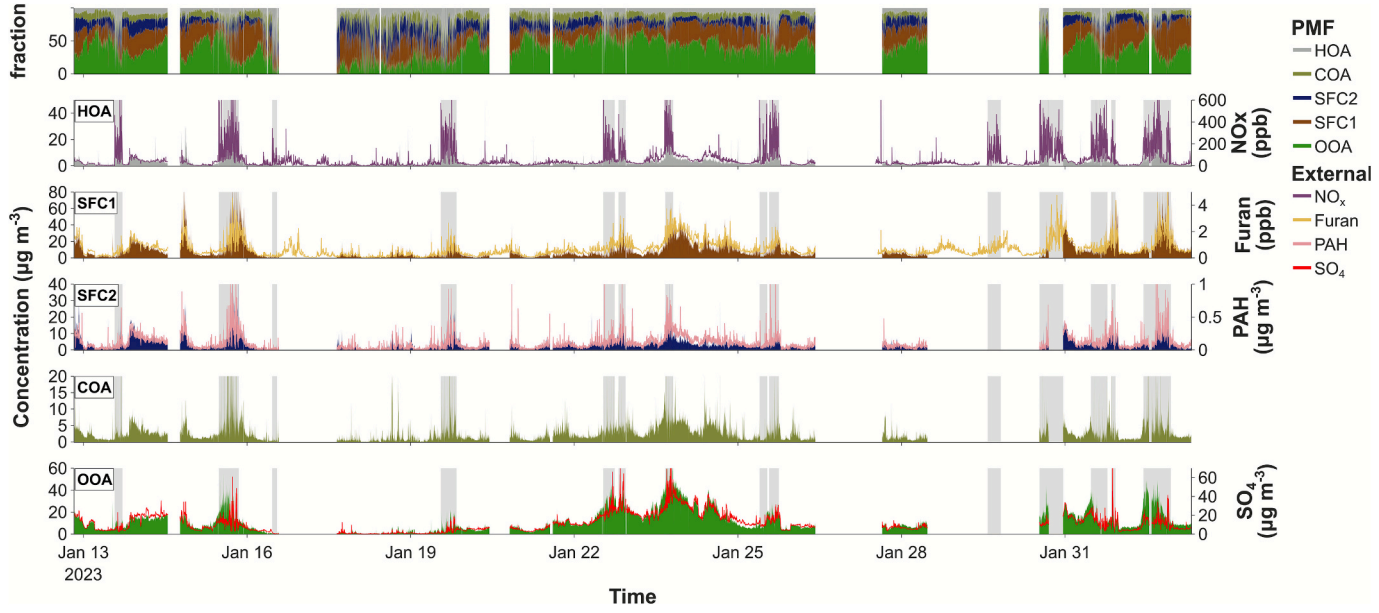

Fig. 4. Timeseries of the identified OA factors (left axis) and respective external tracers (right axis) over the total measurement period. Grey shading indicates periods of mobile measurements. The top panel represents the timeseries of the relative contribution of all factors.

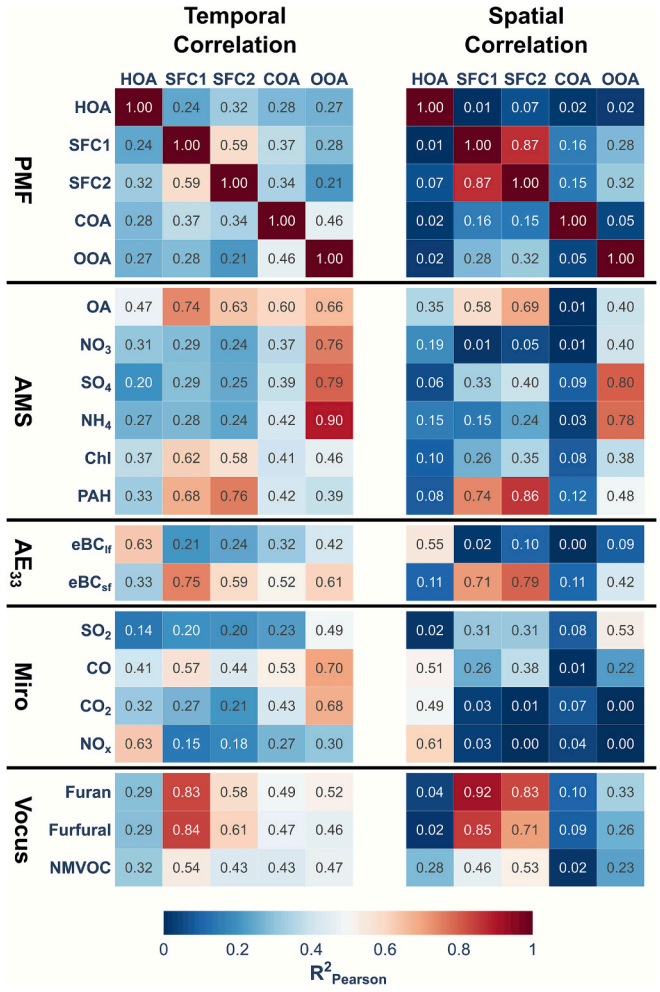

Fig. 5. Correlation Matrix of PMF factors with collocated measurements in the mobile lab on a temporal (left) and spatial (right) scale.

et al., 2015; Ng et al., 2010). O/C ratios in this study are calculated using the Improved-Ambient method by Canagaratna et al. (2015), which shows ~30 % higher values compared to the older Aiken-Ambient method still used in older publications. Fig. 4 shows the significant increase of HOA during times of mobile measurements, mainly due to short term plumes of traffic exhaust. Correlation of the HOA factor with nitrogen oxides (NO_x(g)=NO(g) + NO_2(g)), as well as equivalent black carbon apportioned to liquid fuel (eBC_{lf}), show linear dependence, both on a temporal and spatial scale (R^2 of 0.63/0.61 and 0.63/0.55, respectively), significantly higher than all other factors, where no notable correlation of these factors with NO_x(g) and eBC_{lf} could be found, specifically on a spatial scale.

The two SFC factors are mainly associated with domestic heating, with SFC1 and SFC2 related to more and less efficient combustion, respectively. SFC1 shows high contributions of $C_2H_4O_2^+$ (*m/z* 60) and $C_3H_5O_2^+$ (*m/z* 73) which are tracers of biomass burning emissions stemming from fragmentation of anhydrosugars such as levoglucosan (Alfarra et al., 2007). The fraction of these tracers ($f_{C_2H_4O_2^+}$ = 0.026, $f_{C_3H_5O_2^+}$ = 0.013) are comparable to other typical biomass burning factors (BBOA) at urban stations (Chen et al., 2022; Crippa et al., 2014). While the majority of the factor is influenced by ion fragments containing only carbon and hydrogen (CH) or additionally one oxygen atom (CHO) at lower masses, masses at high *m/z* ratios contribute 14 % of the total factor, including detectable signals from PAHs (Dzepina et al., 2007). The diurnal pattern of the SFC1 factor shows an increase in the evening during the onset of residential heating period (Fig. S11). As discussed later, the spatial distribution of the two SFC factors is also consistent with domestic heating patterns.

SFC2 shows a similar spatial (R^2 = 0.87) and diurnal trend (R^2 = 0.92) to SFC1. However, the two factors are clearly separated in the PMF with 4 or more factors and do not show mixing. The mass spectrum of SFC2 is characterized by increased influence of fragments from unsaturated hydrocarbons and PAHs at *m/z* 91 ($C_7H_7^+$), 115 ($C_9H_7^+$), 202 or 252 and shows a lack of the aforementioned tracers for BBOA emissions ($C_2H_4O_2^+$, $C_3H_5O_2^+$). This factor overall is mainly influenced by CH fragments and shows little oxygenation, with contributions from CHO1 fragments at 9 % and CHOgt1 (CH with more than one oxygen atom) at 3 %. Additionally, UMR masses above *m/z* 120 contribute >30 % to the factor, with an increased contribution at *m/z* ratios identified for typical PAHs in Dzepina et al. (2007) or Bruns et al. (2015). These features are similar to coal combustion factors (CCOA) determined in other studies (Dall'Osto et al., 2013; Elser et al., 2016b; Hu et al., 2016; Tong et al., 2021). In the present study, this would indicate residential coal combustion since there are no large-scale industrial sources present in the city of Sarajevo. Coal combustion should typically be accompanied by Chl or SO_2(g) emissions (Tobler et al., 2021). No significant correlation, however, of SFC2 with SO_2(g) could be found including for days having low influence from regional transport, when possible influences of industrial emissions from outside of Sarajevo on SO_2(g) would be minimized. The correlation with Chl is somewhat higher at R^2 = 0.58, however a similar correlation of Chl is also found for SFC1 (R^2 = 0.62). Therefore, we cannot exclude the influence and contribution of other low-efficiency combustion sources. The strongest correlation of SFC2 is found with PAHs (R^2 = 0.76 temporal/R^2 = 0.86 spatial). However, high PAH content alone is insufficient to assign this factor to coal; Bruns et al. (2015) demonstrated that inefficient wood combustion in a domestic heating appliance can also generate OA with high PAH content and additionally strongly decreased $f_{C_2H_4O_2^+}$. Therefore, we adopt a conservative interpretation of this factor and assign it to low-efficiency combustion, which may encompass a combination of different fuel types, appliances, and/or operation, similar to other studies (Lalchandani et al., 2021; Tobler et al., 2020; Young et al., 2015).

Both factors show high correlation with the VOCs furan(g) and furfural(g) respectively, two known tracers of biomass burning emissions (Bruns et al., 2017; Gilman et al., 2015), with SFC1 being stronger correlated than SFC2. eBC_{sf} also shows a good correlation with SFC1 on the temporal scale (R^2 = 0.75), while on a spatial scale SFC2 exhibits an even slightly higher correlation (R^2 = 0.79). This is due to both factors, while different in chemistry, being associated with the same source of domestic heating, which is concentrated in residential areas and thus spatially correlated, also explaining their overall high correlation.

The fourth factor, COA, is another primary source of particulate matter, related to cooking emissions. The mass spectrum has a similar pattern as the HOA factor but has more pronounced contributions from select species (e.g. $C_3H_3O^+$, $C_2H_3O^+$) that have been shown to originate from the oxygenation of fatty acids and increased ratios of *m/z* 41/43 and *m/z* 55/57 (Huang et al., 2010; Mohr et al., 2012). While no significant correlations of this factor with tracers from external measurements were determined, the diurnal cycle of COA during stationary measurements shows peaks around 14:00 and 21:00 local time (LT), which corresponds roughly to typical mealtimes. As mentioned though, the diurnal cycle should be considered with caution and more weight is put to the spatial distribution for the identification of this factor, presented in the following section.

In comparison to the other factors, OOA shows the highest O/C ratio (0.59). It is of secondary origin associated with gas-phase precursors as well as aging processes as evidenced by the increased contribution of oxygenated species that results in substantially enhanced signal for CO_2^+. OOA could not be further separated into more- or less-oxygenated fraction, as has been observed before for wintertime campaigns (Zhang et al., 2011). With ratios for $f_{CO_2^+}$ = 0.09 and $f_{C_2H_3O^+}$ = 0.05,

these measurements lie in the lower end of the range for typical combined OOA and more closely resemble less oxidized-oxygenated OA (LO-OOA) (Chen et al., 2022; Ng et al., 2010), indicating a large influence of primary emissions in Sarajevo. The diurnal cycle of OOA shows a slight increase during early afternoon hours, while staying relatively flat throughout the day. This increase, however, seems affected by missing time in the stationary measurements due to mobile sampling (Fig. S11). OOA shows its highest correlation with the inorganic compounds measured by the AMS (NO_3: $R^2 = 0.76$, SO_4: $R^2 = 0.79$, NH_4: $R^2 = 0.90$), suggesting that this factor is largely influenced by meteorology and regional transport (Fröhlich et al., 2015). Interestingly, while SO_4 and NH_4 also show high spatial correlations, the spatial correlation with NO_3 is clearly weaker, suggesting that its association is driven more by meteorological conditions (see Section 3.3).

The timeseries of the contribution of the five factors to the overall OA mass (Fig. 4) shows distinct variability at the beginning and end of the campaign, whereas the period between January, 22–25 exhibits relatively little variation, likely due to the buildup and accumulation of both primary and secondary species under stagnant conditions. Notable increases in the fraction of SFC at the start and end of the campaign correspond to a decrease in the fraction of OOA, while the HOA and COA fractions remain at a consistent level. Although the fraction of OOA decreases during these times, its absolute concentration still increases, but to a lesser extent than the overall OA. This indicates an increasing dominance of SFC at higher OA concentrations, as is also seen in Fig. S12, specifically for times of mobile measurements.

Fig. 6 presents a breakdown of the measured NR-PM_1 + eBC composition and source apportionment results for stationary and mobile measurement periods. Mean concentrations during mobile measurement periods are more than twice as high as during stationary measurements (99.4 $\mu g\, m^{-3}$ vs. 44.1 $\mu g\, m^{-3}$), however the fractional composition does not change significantly. The mobile measurements show an increased contribution from HOA (4.3–10.3 %) and eBC_{lf} (3.1–6.8 %), as expected due to the proximity to individual traffic-related plumes. On the other hand, the average contributions from SO_4 decrease during mobile measurement periods (23.8–16.2 %). This relative reduction may be influenced by the typical timing of mobile measurements, which were conducted during afternoon and evening hours. These periods are more strongly influenced by primary emissions, leading to a relative increase in primary over secondary aerosol components and yielding overall higher concentrations. Overall, this comparison suggests that, when mobile measurements are averaged over the entire city, the chemical composition of PM_1 is broadly comparable to that observed during stationary measurements at the Sarajevo-Bjelave site. However, as demonstrated in the following section, a more detailed analysis of the spatial distribution reveals that this similarity does not apply to all regions across Sarajevo.

3.3. Spatial results

Mobile measurements enable the characterization of the spatial resolution of atmospheric pollution and identification of discrete, localized emission sources. This is particularly important in urban areas, where industrial, residential, and commercial activity can vary significantly over short distances, even at the scale of individual neighborhoods or streets. Fig. 7 depicts concentration maps of the OA factors identified in the previous section, averaged across all measurement days and individual loops to provide a representative map for the one-month period of measurements in the city of Sarajevo. Overall, there is a slight trend of higher OA concentrations in the western part of Sarajevo towards Ilidža while concentrations in the city center are generally lower (Fig. 7a for regional boundaries). A similar spatial distribution is also seen for OOA. In contrast, HOA exhibits distinct pollution spikes along major streets, but does not show an east–west gradient or notable enhancements in specific neighbourhoods. The most significant spatial patterns are associated with the two SFC factors and COA which show

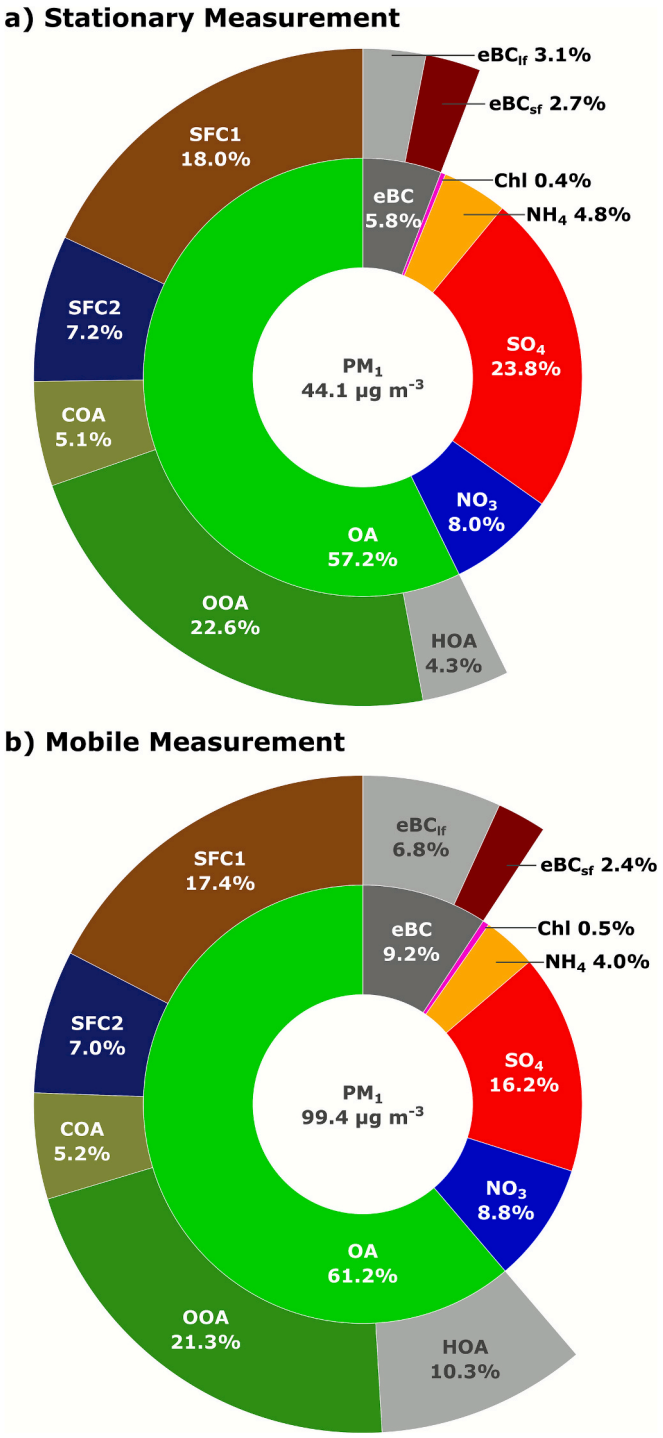

Fig. 6. Chemical composition of the PM_1 mass concentration for averaged (a) stationary- and (b) mobile measurements as well as apportioned contribution of OA and eBC sources to the overall mass.

contrasting spatial distributions. Fig. 7c and d show elevated concentrations of SFC particularly along the North and South Hill and near neighbourhoods along the southern part of the loop in Novo Sarajevo and the northern part of the loop in Novi Grad, areas which are primarily residential with a high number of these houses shown to use wood and coal as a heating source (CETEOR & E3, 2024). SFC (SFC1 + SFC2) contribute up to 50 % of the total OA in these neighborhoods. In contrast, its contribution is significantly lower in the valley and the city center, where houses are connected to the central heating grid. The spatial distribution of measured SFC concentrations overall is consistent

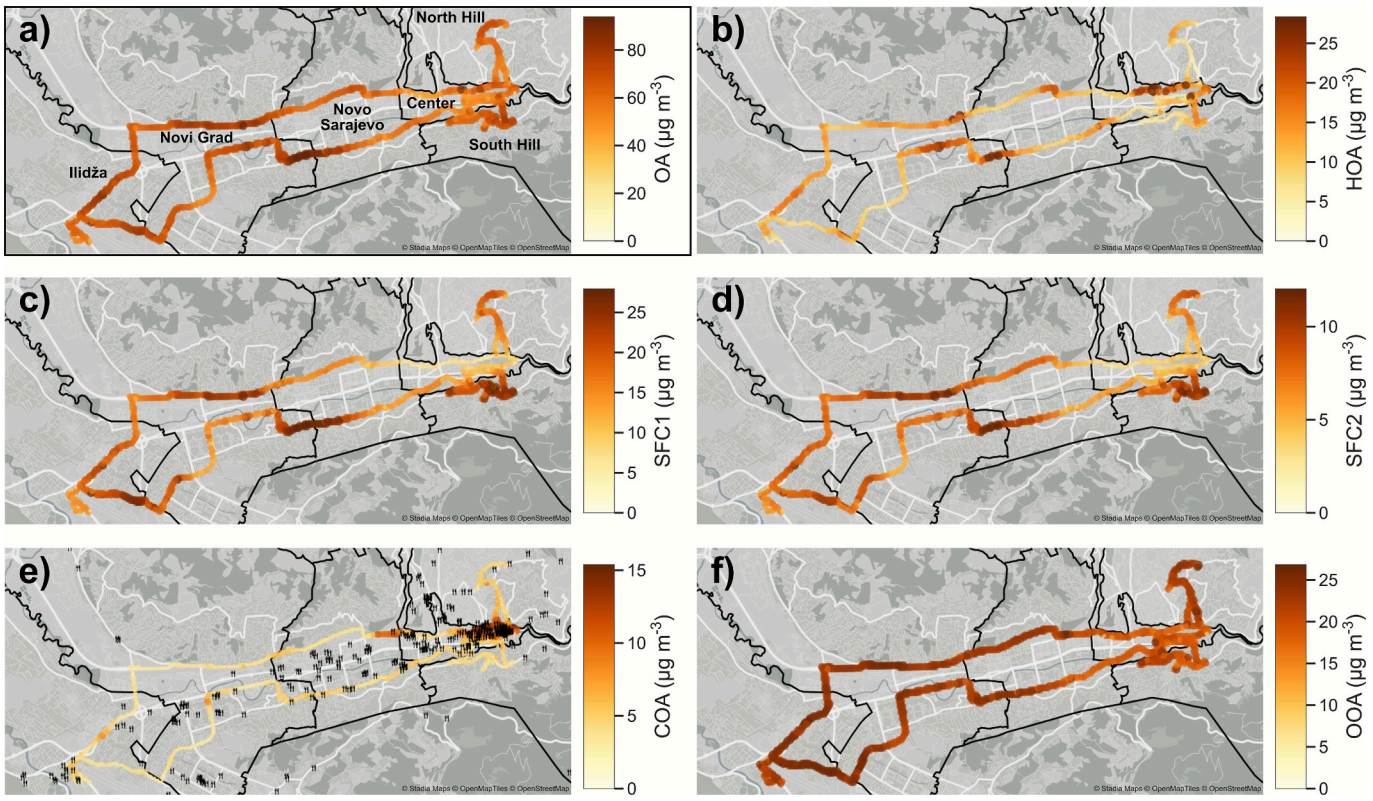

Fig. 7. Averaged spatial concentrations over the entire mobile measurement campaign of organic aerosol and the five determined factors: HOA (b), SFC1 (c), SFC2 (d), COA (e) and OOA (f). Black symbols in e) represent locations of restaurants in Sarajevo (OpenStreetMap data).

with the distribution of residential buildings using solid fuel as a source of heating and of bottom-up emissions estimates from these buildings (CETEOR & E3, 2024; Sarajevo Canton, n.d.). COA emissions, on the other hand, are specifically increased in the city center and valley areas, seemingly influenced by emissions from restaurants. Panel e) of Fig. 7 shows the location of restaurants in the city of Sarajevo (OpenStreetMap), which coincides with areas of increased concentrations of COA. In these regions the relative contribution of COA to total OA reaches up to 30 %.

As mentioned previously, SO_4, NH_4 and SO_2(g) show a linear relation to OOA on a spatial scale (R^2 = 0.80, 0.78, 0.53, respectively) with all components displaying a similar east–west gradient across the city (Fig. 8, Fig. S13). This suggests a regional influence affecting both OOA and these secondary species. NO_3 however, does not follow this trend and shows no enhancement in the Ilidža region in the west of the city, pointing to different formation pathways compared to the other secondary species, most likely due to the differing spatial distribution of SO_2(g) and NO_x(g) as precursor gases. While windspeeds were mostly low during times of mobile measurements, highlighting the overall significance of local emission sources, wind directions in the Ilidža region were also frequently from the west/northwest sectors, bringing air from areas with industrial sources that is likely elevated in SO_2(g). During the same time periods, wind directions at the eastern part of the city (Bjelave site) came mainly from south-east, a rural area with little

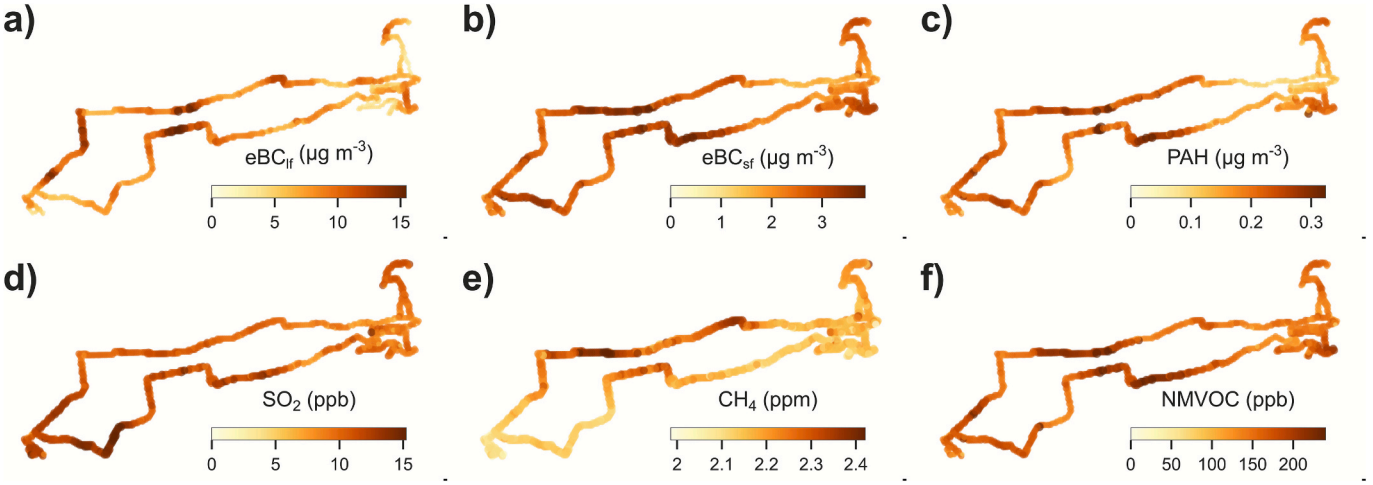

Fig. 8. Spatial concentrations averaged over the entire campaign for eBC_{tr}, eBC_{sf}, PAH, SO_2(g), CH_4(g) and non-methane volatile organic carbon that can be measured by the Vocus (NMVOC(g)).

industrial activity. In contrast, NO_x(g) does not show a similar east-to-west gradient as SO_2(g) due to the distribution of traffic (and combustion) sources. However, given the much coarser temporal resolution of available wind data compared to short time scales of mobile measurement transects at the respective locations, as well as the complex geography of Sarajevo, spatial diagnostics including wind data should be regarded as indicative rather than conclusive.

The spatial distribution of eBC_{lf} (Fig. 8) resembles that of HOA, however lacking the clear concentration spikes seen in the HOA profile in the city center. PAHs distributions closely resembles the SFC factors, highlighting the negative influence of primary combustion sources and their potential health impacts due to the toxic nature of PAHs within the city. A similar distribution is also observed for eBC_{sf}. In contrast, Chl shows a distinct spatial pattern that does not correspond to SFC2, as can be seen in Fig. S13e. As discussed earlier, this suggests that SFC2 emissions are not solely driven by coal combustion but are instead influenced by low efficiency combustion in general.

Several other gas-phase species show spatial patterns that align well with the PMF factors in the particle phase, suggesting they are co-emitted from the same source. For example, furan(g) and furfural(g) follow the same spatial distribution as SFC, while NO_x(g) correlates with the spatial distribution of HOA (Fig. S13f). Non-methane volatile organic carbon (NMVOC(g)) as a whole expectedly does not show strong correlation to any specific source due to diverse VOC(g) source contributions (Fig. 8f). A special case is methane (CH_4(g)), for which elevated concentrations are observed in the central northern part of the loop in Novi Grad (Fig. 8e), but these enhancements appear only in the gas-phase and do not correspond to any of the particle-phase factors. While CH_4 levels in this region are consistently higher on average, the magnitude and exact location of the enhancement vary. This suggests an additional, likely independent gas-phase source in that area that is not reflected in the particulate PMF, potentially due to gas leakages in this area.

To better distinguish temporal trends within the city, the spatial data was divided into two time periods: afternoon (12:00–16:45 LT) and evening (16:45–00:00 LT). Further subdivision into shorter time periods was avoided to maintain statistical relevance. The time 16:45 LT was chosen, as this was close to the average time for sunset during our measurement campaign and it additionally also aligns roughly with the end of the workday, when people are expected to return home and begin heating their homes for the evening. Figs. S14 and S15 show the spatial distribution of the factors for these two time periods while Table S3 contains information on the concentration and composition of the OA in the different regions of Sarajevo during mobile measurements overall and in the afternoon and evening. Concentrations observed during mobile measurements in the afternoons were generally lower (OA = 49.8 ± 31.1 μg m^{-3}) than in the evenings (OA = 80.1 ± 40.0 μg m^{-3}). While changes to height of the planetary boundary layer can have an impact as well, the main driver for this trend is solid fuel combustion, which remains relatively low during the day throughout the city but increases significantly in the evenings, especially in the western part of the city. The importance of this factor and its contribution to air pollution in Sarajevo are illustrated in Fig. 9, where the loop is color-coded by the factor that most frequently shows the highest contribution to the overall OA at each location. While the entire urban area is dominated by the secondary source (OOA) during the afternoon, in the evening primary emissions, mainly from solid fuel combustion (SFC1 + SFC2), account for the highest contributions across nearly the entire city, except for an area around the city center, where OOA and COA contribute most to total OA.

Another trend, primarily observed in the evenings, is a concentration gradient from east to west. Fig. 10 depicts concentrations and compositions for different areas of Sarajevo and compares afternoon and evening values, not only for the five PMF factors of OA but also for inorganic aerosol and eBC. As shown, concentrations and compositions throughout the afternoon vary little between the different regions (PM_1 = 81.3 ± 4.3 μg m^{-3}). However, in the evenings a clear increase in concentrations is observed in the western regions compared to the center, exhibiting a spatial gradient east to west. Concentrations in Ilidža increase to 165.2 μg m^{-3}, while averaged evening PM_1 concentrations in the center are 91.2 μg m^{-3}. Additionally, regions at higher elevations north and south of the center (North Hill and South Hill) also show slight increases. Higher concentrations of SFC and SO_4 explain more than 2/3 of the evening PM_1 increase for Ilidža, Novi Grad and Novo Sarajevo. In contrast, in the eastern part (Center, North Hill, South Hill) almost the entire evening increase in PM_1 is due to SFC and SO_4, as concentrations of other components such as NO_3, NH_4 or OOA show little to no change or are decreasing.

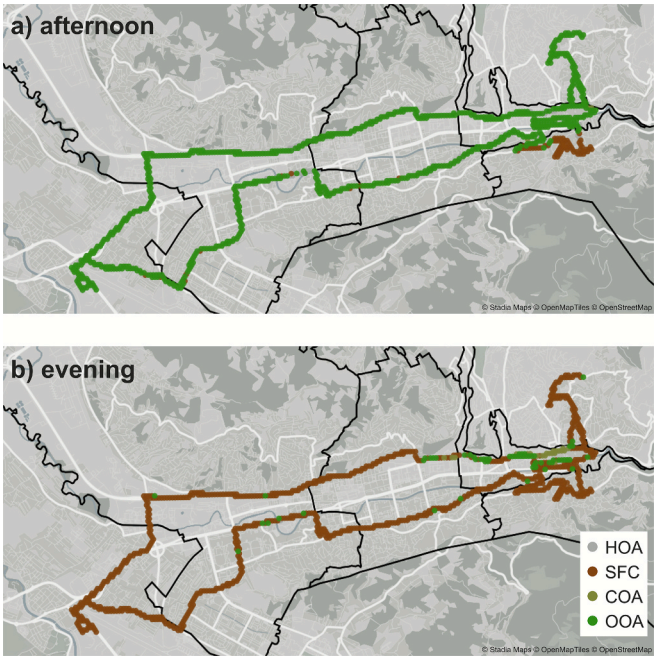

Fig. 9. Spatial distribution of the dominant PMF factors for the (a) afternoon (12:00–16:45) and (b) evening (16:45–00:00) period. Each point is colored according to the factor that most frequently exhibits the highest contribution to total OA at that location.

3.4. Comparison to other European cities

Observed PM_1 concentrations during the one-month campaign of 42.7 μg m^{-3} are higher than usually observed $PM_{2.5}$ measurements in most European countries. Comparing to other measurements within the Southeastern European region these concentrations are high compared to neighboring countries like Croatia but are exceeded frequently within Bosnia and Herzegovina itself and locations in Northern Macedonia (Federal Hydrometeorological Institute Bosnia and Herzegovina, 2024; European Environment Agency (EEA), 2025). Overall though, measurements in the region remain scarce. The relative PM_1 composition based on AMS species in Sarajevo is broadly comparable to other urban measurements at many European measurement sites, with OA contributing 59 % on average. High sulphate contributions (21 % for this study) have been reported previously, however for usually lower concentration compared to 11.4 μg m^{-3} reported here (Bressi et al., 2021; Chen et al., 2022; Crippa et al., 2014). The relative OA composition based on source apportionment results, shows clearly higher importance of primary sources in Sarajevo compared to elsewhere in Europe during winter months (Chen et al., 2022). Especially SFC shows higher contributions in Sarajevo, comparable only to some results for other cities in BiH and North Macedonia (Almeida et al., 2020; Grundström et al., 2022). Contributions from traffic related sources (HOA = 6 %, eBC_{lf} = 4 %)

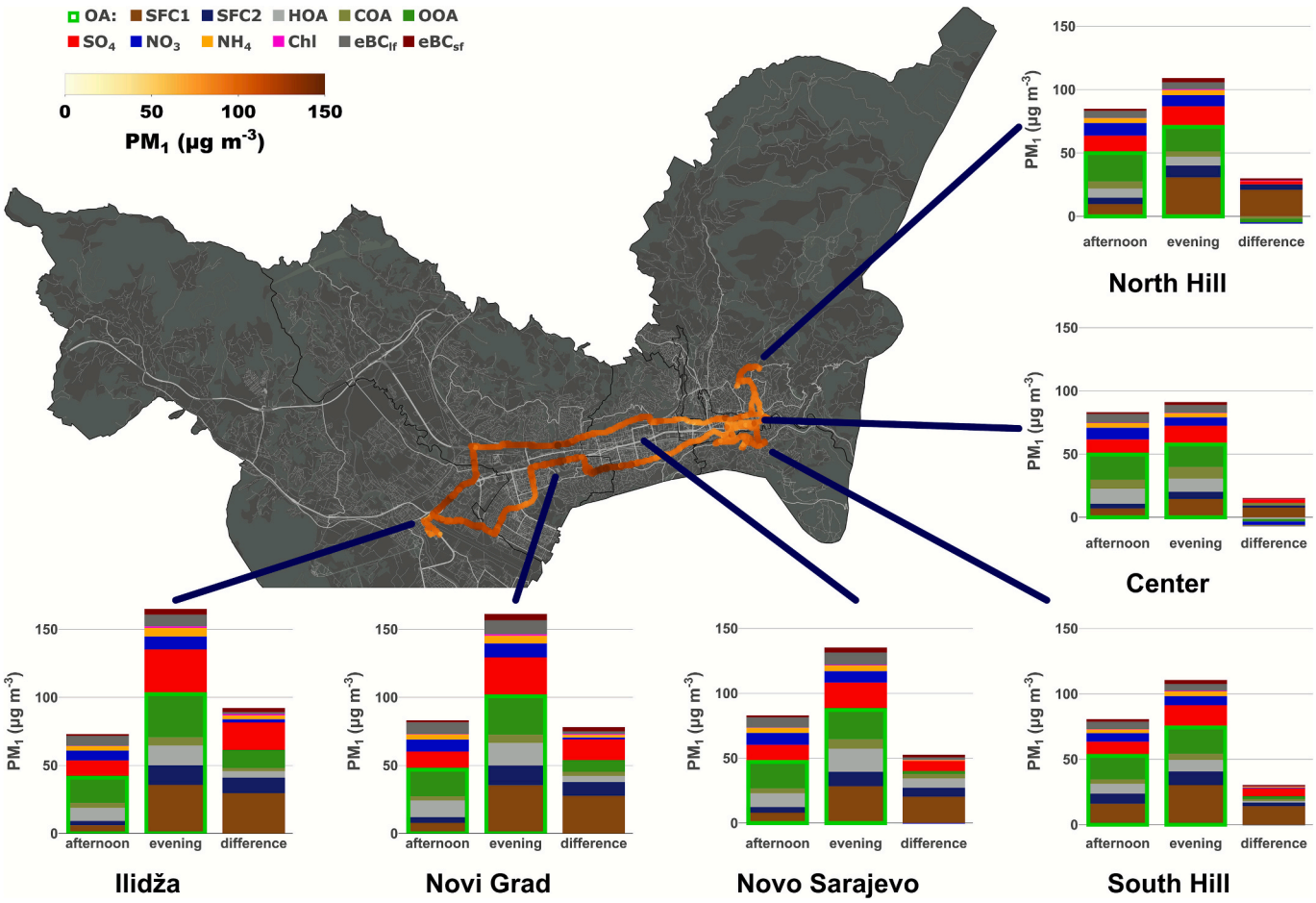

Fig. 10. Afternoon and evening concentrations as well as their difference for all PM_1 species and PMF components for the different regions in Sarajevo.

appear comparable or low in relative terms. In absolute concentrations, however, traffic related sources are in many cases higher than those observed elsewhere (Chen et al., 2022; Crippa et al., 2014) and only appear minor due to the dominance of other sources.

4. Conclusion

These measurements highlight the extent of wintertime air pollution in the city of Sarajevo, with PM_1 concentrations frequently exceeding 100 µg m^{-3} (10 % of data over the entire campaign). Most of this pollution originates from local and primary emissions including traffic (6 % of total PM_1), cooking (6 %), and most notably residential heating especially in evenings ($SFC_{afternoon}$ = 16 %; $SFC_{evening}$ = 32 %). In addition, oxygenated organic aerosol (OOA) from secondary and/or aged OA, plays a notable role (21 %), and is most likely also influenced to a large extent by emissions from residential heating as the main primary organic aerosol source known to be associated with OOA precursors (Grieshop et al., 2009; Heringa et al., 2011).

Observed concentrations during this campaign are higher than reported for other European countries (Chen et al., 2022), with two-thirds of the one-minute measurement data exceeding the WHO 24-hour $PM_{2.5}$ guideline of 15 µg m^{-3}. However, it should be noted that the campaign covers only a one-month period during wintertime when pollution levels are expected to peak. Compared to previous winters, the month captured in this study is broadly representative of typical winter conditions in Sarajevo, with pollution concentrations falling within the range observed in past winters (European Environment Agency (EEA), 2025). As such, this study serves to fill the gap in this understudied but highly polluted European city. The high contribution and concentrations of primary emissions in Sarajevo not only highlight the severity of the pollution, but from a mitigation perspective suggest that strategies to curb emissions can be effective as primary sources are more easily identifiable and controllable compared to secondary pollutants.

The use of mobile measurements allowed the resolution of clear spatial differences in air pollution across Sarajevo. While COA overall contributes 6 % to PM_1 on average, this fraction increases to 9 % in the city center. Conversely, emissions from solid fuel combustion are reduced in the center but play a crucial role in all other measured regions of the city, mainly around residential areas, and especially in the evenings. During these hours a pronounced east-to-west concentration gradient is observed, driven by primary organic aerosol (mainly SFC), and influenced by local meteorological conditions, including downslope winds and air being likely pushed westwards out of the valley leading to accumulation of pollution in the basin around Ilidža. The co-emission of toxic pollutants such as PAHs, particularly from lower-efficiency combustion or possible coal influence (SFC2), further highlights the importance of these sources for local air quality and public health.

The contribution of SFC-related emissions increases with rising OA concentrations, indicating that reducing emissions from this source could have a large impact on overall pollution levels. Targeting these emissions may also help to reduce the toxicity of air pollution due to the associated reduction of PAHs. These results therefore confirm the current strategy and main focus in the Canton Sarajevo on reducing emissions from residential heating by introducing measures to limit the use of residential heating (CETEOR & E3, 2024). However, based on the current goal of reducing SFC-related emissions by 90 %, these results would suggest that air pollution in Sarajevo during winter times would still remain high, even under the assumption that a significant part of the

OOA is driven by solid fuel combustion. While traffic is the second clear target for reducing emissions, COA especially in the city center was shown to have a notable contribution to the pollution on a mostly local scale, however in an area with dense population. Overall it is important to highlight, that due to the city's complex topography and distribution of residential areas, where individual household heating is dominant, not all areas are affected equally. This underlines the value and importance spatially resolved data can bring for evaluating air pollution exposure and developing location-specific mitigation strategies.

CRediT authorship contribution statement

Michael Bauer: Writing – review & editing, Writing – original draft, Visualization, Methodology, Investigation, Formal analysis, Data curation. **Jay G. Slowik:** Writing – review & editing, Supervision, Methodology, Investigation. **Marta Via:** Writing – review & editing, Investigation. **Peeyush Khare:** Writing – review & editing, Investigation. **Benjamin Chazeau:** Writing – review & editing, Investigation. **Kristina Glojek:** Writing – review & editing, Investigation. **Manousos Manousakas:** Writing – review & editing, Investigation. **Zachary C.J. Decker:** Writing – review & editing, Investigation. **Asta Gregorič:** Writing – review & editing, Investigation. **Almir Bijedić:** Writing – review & editing, Resources. **Enis Krečinić:** Writing – review & editing, Investigation. **Griša Močnik:** Writing – review & editing, Resources, Project administration, Investigation, Funding acquisition, Conceptualization. **Katja Džepina:** Writing – review & editing, Project administration, Investigation, Funding acquisition, Conceptualization. **André S. H. Prévôt:** Writing – review & editing, Supervision, Resources, Project administration, Methodology, Investigation, Funding acquisition, Conceptualization.

Funding

This work was supported by the Swiss Federal Office for the Environment, Switzerland, ARIS program P1-0385, and the SAAERO project (EU H2020 MSCA-IF 2020 [grant number 101028909]). MV acknowledges SMASH (EU Horizon MSCA-COFUND under the grant agreement No. 101081355, R Slovenia and the European Union from the European Regional Development Fund).

Declaration of competing interest

The authors declare the following financial interests/personal relationships which may be considered as potential competing interests: At the time of the research, Asta Gregorič was employed by Aerosol d.o.o., the manufacturer of Aethalometer instruments also used in this study. The company had no role in study design, data collection and analysis, decision to publish, or preparation of the manuscript. All other authors have no conflict of interest to disclose.

Acknowledgement

We thank all the participants and collaborators involved in the SAAERO campaign for their support and contributions. Special thanks go to the technicians (Pascal Schneider, Levi Folghera) who helped set up the mobile laboratory and supported the driving.

Map visualisations were produced using map tiles from Stadia Maps (stadiamaps.com), OpenMapTiles (https://openmaptiles.org) and ©OpenStreetMap contributors, available under the Open Database License (https://www.openstreetmap.org/copyright). We acknowledge the use of SRTM elevation data in Fig. 1 (Farr et al., 2007; Farr and Kobrick, 2000; NASA Shuttle Radar Topography Mission (SRTM), 2013) distributed by OpenTopography (https://opentopography.org/).

Appendix A. Supplementary data

Supplementary data to this article can be found online at https://doi.org/10.1016/j.envint.2025.110009.

Data availability

The full dataset used in the figures is publicly available under https://doi.org/10.5281/zenodo.17961367.

References

Agency for Statistics of Bosnia and Herzegovina, 2015. Survey on Houshold Energy Consumption in BiH. Agency for Statistics of Bosnia and Herzegovina, Sarajevo, BiH.

Alfarra, M.R., Prevot, A.S.H., Szidat, S., Sandradewi, J., Weimer, S., Lanz, V.A., Schreiber, D., Mohr, M., Baltensperger, U., 2007. Identification of the mass spectral signature of organic aerosols from wood burning emissions. Environ. Sci. Technol. 41, 5770–5777. https://doi.org/10.1021/es062289b.

Allan, J.D., Jimenez, J.L., Williams, P.I., Alfarra, M.R., Bower, K.N., Jayne, J.T., Coe, H., Worsnop, D.R., 2003. Quantitative sampling using an Aerodyne aerosol mass spectrometer 1. Techniques of data interpretation and error analysis. J. Geophys. Res. Atmosph. 108. https://doi.org/10.1029/2002JD002358.

Almeida, S.M., Manousakas, M., Diapouli, E., Kertesz, Z., Samek, L., Hristova, E., Šega, K., Alvarez, R.P., Belis, C.A., Eleftheriadis, K., 2020. Ambient particulate matter source apportionment using receptor modelling in European and Central Asia urban areas. Environ. Pollut. 266, 115199. https://doi.org/10.1016/j.envpol.2020.115199.

Belis, C.A., Matkovic, V., Ballocci, M., Jevtic, M., Millo, G., Mata, E., Van Dingenen, R., 2023. Assessment of health impacts and costs attributable to air pollution in urban areas using two different approaches. a case study in the Western Balkans. Environ. Int. 182, 108347. https://doi.org/10.1016/j.envint.2023.108347.

Bosnia and Herzegovina Automobile and Motorcycle Club, 2023. Information on registered motor vehicles in Bosnia and Herzegovina in the period January-December 2022.

Bressi, M., Cavalli, F., Putaud, J.P., Fröhlich, R., Petit, J.-E., Aas, W., Äijälä, M., Alastuey, A., Allan, J.D., Aurela, M., Berico, M., Bougiatioti, A., Bukowiecki, N., Canonaco, F., Crenn, V., Dusanter, S., Ehn, M., Elsasser, M., Flentje, H., Graf, P., Green, D.C., Heikkinen, L., Hermann, H., Holzinger, R., Hueglin, C., Keernik, H., Kiendler-Scharr, A., Kubelová, L., Lunder, C., Maasikmets, M., Makeš, O., Malaguti, A., Mihalopoulos, N., Nicolas, J.B., O'Dowd, C., Ovadnevaite, J., Petralia, E., Poulain, L., Priestman, M., Riffault, V., Ripoll, A., Schlag, P., Schwarz, J., Sciare, J., Slowik, J., Sosedova, Y., Stavroulas, I., Teinemaa, E., Via, M., Vodička, P., Williams, P.I., Wiedensohler, A., Young, D.E., Zhang, S., Favez, O., Minguillón, M.C., Prevot, A.S.H., 2021. A European aerosol phenomenology - 7: high-time resolution chemical characteristics of submicron particulate matter across Europe. Atmos. Environ.: X 10, 100108. https://doi.org/10.1016/j.aeaoa.2021.100108.

Bruns, E.A., Krapf, M., Orasche, J., Huang, Y., Zimmermann, R., Drinovec, L., Močnik, G., El-Haddad, I., Slowik, J.G., Dommen, J., Baltensperger, U., Prévôt, A.S.H., 2015. Characterization of primary and secondary wood combustion products generated under different burner loads. Atmosph. Chem. Phys. 15, 2825–2841. https://doi.org/10.5194/acp-15-2825-2015.

Bruns, E.A., Slowik, J.G., El Haddad, I., Kilic, D., Klein, F., Dommen, J., Temime-Roussel, B., Marchand, N., Baltensperger, U., Prévôt, A.S.H., 2017. Characterization of gas-phase organics using proton transfer reaction time-of-flight mass spectrometry: fresh and aged residential wood combustion emissions. Atmosph. Chem. Phys. 17, 705–720. https://doi.org/10.5194/acp-17-705-2017.

Bukowiecki, N., Dommen, J., Prévôt, A.S.H., Richter, R., Weingartner, E., Baltensperger, U., 2002. A mobile pollutant measurement laboratory—measuring gas phase and aerosol ambient concentrations with high spatial and temporal resolution. Atmos. Environ. 36, 5569–5579. https://doi.org/10.1016/S1352-2310(02)00694-5.

Canagaratna, M.R., Jimenez, J.L., Kroll, J.H., Chen, Q., Kessler, S.H., Massoli, P., Hildebrandt Ruiz, L., Fortner, E., Williams, L.R., Wilson, K.R., Surratt, J.D., Donahue, N.M., Jayne, J.T., Worsnop, D.R., 2015. Elemental ratio measurements of organic compounds using aerosol mass spectrometry: characterization, improved calibration, and implications. Atmosph. Chem. Phys. 15, 253–272. https://doi.org/10.5194/acp-15-253-2015.

Canonaco, F., Crippa, M., Slowik, J.G., Baltensperger, U., Prévôt, A.S.H., 2013. SoFi, an IGOR-based interface for the efficient use of the generalized multilinear engine (ME-2) for the source apportionment: ME-2 application to aerosol mass spectrometer data. Atmosph. Meas. Tech. 6, 3649–3661. https://doi.org/10.5194/amt-6-3649-2013.

Canonaco, F., Tobler, A., Chen, G., Sosedova, Y., Slowik, J.G., Bozzetti, C., Daellenbach, K.R., El Haddad, I., Crippa, M., Huang, R.-J., Furger, M., Baltensperger, U., Prévôt, A.S.H., 2021. A new method for long-term source apportionment with time-dependent factor profiles and uncertainty assessment using SoFi pro: application to 1 year of organic aerosol data. Atmosph. Meas. Tech. 14, 923–943. https://doi.org/10.5194/amt-14-923-2021.

Canton Sarajevo, n.d.. KVALITET ZRAKA | Registar emisija u zrak (AIR QUALITY | Air Emissions Register). https://digitalnaplatforma.ks.gov.ba/portal/apps/dashboards/93f0f8429cb94336ba2e427488695950 (Accessed: 10.23.25).

CETEOR & E3, 2024. Strategy for Limiting the Use of Coal and Other Solid Fuels in Sarajevo Canton (2023–2033). United Nations Development Programme, Sarajevo, BiH. https://www.undp.org/bosnia-herzegovina/publications/strategy-limiting-use-coal-and-other-solid-fuels-sarajevo-canton-2023-2033-executive-summary.

Chen, G., Canonaco, F., Tobler, A., Aas, W., Alastuey, A., Allan, J., Atabakhsh, S., Aurela, M., Baltensperger, U., Bougiatioti, A., De Brito, J.F., Ceburnis, D., Chazeau, B., Chebaicheb, H., Daellenbach, K.R., Ehn, M., El Haddad, I., Eleftheriadis, K., Favez, O., Flentje, H., Font, A., Fossum, K., Freney, E., Gini, M., Green, D.C., Heikkinen, L., Herrmann, H., Kalogridis, A.-C., Keernik, H., Lhotka, R., Lin, C., Lunder, C., Maasikmets, M., Manousakas, M.I., Marchand, N., Marin, C., Marmureanu, L., Mihalopoulos, N., Močnik, G., Nęcki, J., O'Dowd, C., Ovadnevaite, J., Peter, T., Petit, J.-E., Pikridas, M., Matthew Platt, S., Pokorná, P., Poulain, L., Priestman, M., Riffault, V., Rinaldi, M., Różański, K., Schwarz, J., Sciare, J., Simon, L., Skiba, A., Slowik, J.G., Sosedova, Y., Stavroulas, I., Styszko, K., Teinemaa, E., Timonen, H., Tremper, A., Vasilescu, J., Via, M., Vodička, P., Wiedensohler, A., Zografou, O., Cruz Minguillón, M., Prévôt, A.S.H., 2022. European aerosol phenomenology – 8: Harmonised source apportionment of organic aerosol using 22 Year-long ACSM/AMS datasets. Environ. Int. 166, 107325. https://doi.org/10.1016/j.envint.2022.107325.

Cheung, R.K.Y., Qi, L., Manousakas, M.I., Puthussery, J.V., Zheng, Y., Koenig, T.K., Cui, T., Wang, T., Ge, Y., Wei, G., Kuang, Y., Sheng, M., Cheng, Z., Li, A., Li, Z., Ran, W., Xu, W., Zhang, R., Han, Y., Wang, Q., Wang, Z., Sun, Y., Cao, J., Slowik, J. G., Dällenbach, K.R., Verma, V., Gysel-Beer, M., Qiu, X., Chen, Q., Shang, J., El-Haddad, I., Prévôt, A.S.H., Modini, R.L., 2024. Major source categories of PM2.5 oxidative potential in wintertime Beijing and surroundings based on online dithiothreitol-based field measurements. Sci. Total Environ. 928, 172345. https://doi.org/10.1016/j.scitotenv.2024.172345.

Coggon, M.M., Gkatzelis, G.I., McDonald, B.C., Gilman, J.B., Schwantes, R.H., Abuhassan, N., Aikin, K.C., Arend, M.F., Berkoff, T.A., Brown, S.S., Campos, T.L., Dickerson, R.R., Gronoff, G., Hurley, J.F., Isaacman-VanWertz, G., Koss, A.R., Li, M., McKeen, S.A., Moshary, F., Peischl, J., Pospisilova, V., Ren, X., Wilson, A., Wu, Y., Trainer, M., Warneke, C., 2021. Volatile chemical product emissions enhance ozone and modulate urban chemistry. Proc. Natl. Acad. Sci. 118, e2026653118. https://doi.org/10.1073/pnas.2026653118.

Cohen, A.J., Brauer, M., Burnett, R., Anderson, H.R., Frostad, J., Estep, K., Balakrishnan, K., Brunekreef, B., Dandona, L., Dandona, R., Feigin, V., Freedman, G., Hubbell, B., Jobling, A., Kan, H., Knibbs, L., Liu, Y., Martin, R., Morawska, L., Pope, C.A., Shin, H., Straif, K., Shaddick, G., Thomas, M., van Dingenen, R., van Donkelaar, A., Vos, T., Murray, C.J.L., Forouzanfar, M.H., 2017. Estimates and 25-year trends of the global burden of disease attributable to ambient air pollution: an analysis of data from the Global Burden of Diseases Study 2015. Lancet 389, 1907–1918. https://doi.org/10.1016/S0140-6736(17)30505-6.

Crippa, M., Canonaco, F., Lanz, V.A., Äijälä, M., Allan, J.D., Carbone, S., Capes, G., Ceburnis, D., Dall'Osto, M., Day, D.A., DeCarlo, P.F., Ehn, M., Eriksson, A., Freney, E., Hildebrandt Ruiz, L., Hillamo, R., Jimenez, J.L., Junninen, H., Kiendler-Scharr, A., Kortelainen, A.-M., Kulmala, M., Laaksonen, A., Mensah, A.A., Mohr, C., Nemitz, E., O'Dowd, C., Ovadnevaite, J., Pandis, S.N., Petäjä, T., Poulain, L., Saarikoski, S., Sellegri, K., Swietlicki, E., Tiitta, P., Worsnop, D.R., Baltensperger, U., Prévôt, A.S.H., 2014. Organic aerosol components derived from 25 AMS data sets across Europe using a consistent ME-2 based source apportionment approach. Atmosph. Chem. Phys. 14, 6159–6176. https://doi.org/10.5194/acp-14-6159-2014.

Crippa, M., DeCarlo, P.F., Slowik, J.G., Mohr, C., Heringa, M.F., Chirico, R., Poulain, L., Freutel, F., Sciare, J., Cozic, J., Di Marco, C.F., Elsasser, M., Nicolas, J.B., Marchand, N., Abidi, E., Wiedensohler, A., Drewnick, F., Schneider, J., Borrmann, S., Nemitz, E., Zimmermann, R., Jaffrezo, J.-L., Prévôt, A.S.H., Baltensperger, U., 2013. Wintertime aerosol chemical composition and source apportionment of the organic fraction in the metropolitan area of Paris. Atmosph. Chem. Phys. 13, 961–981. https://doi.org/10.5194/acp-13-961-2013.

Daellenbach, K.R., Uzu, G., Jiang, J., Cassagnes, L.-E., Leni, Z., Vlachou, A., Stefenelli, G., Canonaco, F., Weber, S., Segers, A., Kuenen, J.J.P., Schaap, M., Favez, O., Albinet, A., Aksoyoglu, S., Dommen, J., Baltensperger, U., Geiser, M., El Haddad, I., Jaffrezo, J.-L., Prévôt, A.S.H., 2020. Sources of particulate-matter air pollution and its oxidative potential in Europe. Nature 587, 414–419. https://doi.org/10.1038/s41586-020-2902-8.

Dall'Osto, M., Ovadnevaite, J., Ceburnis, D., Martin, D., Healy, R.M., O'Connor, I.P., Kourtchev, I., Sodeau, J.R., Wenger, J.C., O'Dowd, C., 2013. Characterization of urban aerosol in Cork city (Ireland) using aerosol mass spectrometry. Atmosph. Chem. Phys. 13, 4997–5015. https://doi.org/10.5194/acp-13-4997-2013.

De Pieri, S., Arruti, A., Huremovic, J., Sulejmanovic, J., Selovic, A., Đorđević, D., Fernández-Olmo, I., Gambaro, A., 2014. PAHs in the urban air of Sarajevo: levels, sources, day/night variation, and human inhalation risk. Environ. Monit. Assess. 186, 1409–1419. https://doi.org/10.1007/s10661-013-3463-1.

DeCarlo, P.F., Kimmel, J.R., Trimborn, A., Northway, M.J., Jayne, J.T., Aiken, A.C., Gonin, M., Fuhrer, K., Horvath, T., Docherty, K.S., Worsnop, D.R., Jimenez, J.L., 2006. Field-deployable, high-resolution, time-of-flight aerosol mass spectrometer. Anal. Chem. 78, 8281–8289. https://doi.org/10.1021/ac061249n.

Docherty, K.S., Aiken, A.C., Huffman, J.A., Ulbrich, I.M., DeCarlo, P.F., Sueper, D., Worsnop, D.R., Snyder, D.C., Peltier, R.E., Weber, R.J., Grover, B.D., Eatough, D.J., Williams, B.J., Goldstein, A.H., Ziemann, P.J., Jimenez, J.L., 2011. The 2005 Study of Organic Aerosols at Riverside (SOAR-1): instrumental intercomparisons and fine particle composition. Atmosph. Chem. Phys. 11, 12387–12420. https://doi.org/10.5194/acp-11-12387-2011.

Dockery, D.W., Pope, C.A., Xu, X., Spengler, J.D., Ware, J.H., Fay, M.E., Ferris, B.G., Speizer, F.E., 1993. An association between air pollution and mortality in six U.S. Cities. N. Engl. J. Med. 329, 1753–1759. https://doi.org/10.1056/NEJM199312093292401.

Drinovec, L., Močnik, G., Zotter, P., Prévôt, A.S.H., Ruckstuhl, C., Coz, E., Rupakheti, M., Sciare, J., Müller, T., Wiedensohler, A., Hansen, A.D.A., 2015. The "dual-spot" Aethalometer: an improved measurement of aerosol black carbon with real-time loading compensation. Atmosph. Meas. Tech. 8, 1965–1979. https://doi.org/10.5194/amt-8-1965-2015.

Drinovec, L., Jagodič, U., Pirker, L., Škarabot, M., Kurtjak, M., Vidović, K., Ferrero, L., Visser, B., Röhrbein, J., Weingartner, E., Kalbermatter, D.M., Vasilatou, K., Bühlmann, T., Pascale, C., Müller, T., Wiedensohler, A., Močnik, G., 2022. A dual-wavelength photothermal aerosol absorption monitor: design, calibration and performance. Atmosph. Meas. Tech. 15, 3805–3825. https://doi.org/10.5194/amt-15-3805-2022.

Dzepina, K., Arey, J., Marr, L.C., Worsnop, D.R., Salcedo, D., Zhang, Q., Onasch, T.B., Molina, L.T., Molina, M.J., Jimenez, J.L., 2007. Detection of particle-phase polycyclic aromatic hydrocarbons in Mexico City using an aerosol mass spectrometer. Int. J. Mass Spectrom. 263, 152–170. https://doi.org/10.1016/j.ijms.2007.01.010.

Efron, B., 1979. Bootstrap methods: another look at the Jackknife. Ann. Stat. 7, 1–26. https://doi.org/10.1214/aos/1176344552.

Elser, M., Bozzetti, C., El-Haddad, I., Maasikmets, M., Teinemaa, E., Richter, R., Wolf, R., Slowik, J.G., Baltensperger, U., Prévôt, A.S.H., 2016a. Urban increments of gaseous and aerosol pollutants and their sources using mobile aerosol mass spectrometry measurements. Atmosph. Chem. Phys. 16, 7117–7134. https://doi.org/10.5194/acp-16-7117-2016.

Elser, M., Huang, R.-J., Wolf, R., Slowik, J.G., Wang, Q., Canonaco, F., Li, G., Bozzetti, C., Daellenbach, K.R., Huang, Y., Zhang, R., Li, Z., Cao, J., Baltensperger, U., El-Haddad, I., Prévôt, A.S.H., 2016b. New insights into $PM_{2.5}$ chemical composition and sources in two major cities in China during extreme haze events using aerosol mass spectrometry. Atmosph. Chem. Phys. 16, 3207–3225. https://doi.org/10.5194/acp-16-3207-2016.

Elser, M., El-Haddad, I., Maasikmets, M., Bozzetti, C., Wolf, R., Ciarelli, G., Slowik, J.G., Richter, R., Teinemaa, E., Hüglin, C., Baltensperger, U., Prévôt, A.S.H., 2018. High contributions of vehicular emissions to ammonia in three European cities derived from mobile measurements. Atmos. Environ. 175, 210–220. https://doi.org/10.1016/j.atmosenv.2017.11.030.

Eriksson, A.C., Nordin, E.Z., Nyström, R., Pettersson, E., Swietlicki, E., Bergvall, C., Westerholm, R., Boman, C., Pagels, J.H., 2014. Particulate PAH emissions from residential biomass combustion: time-resolved analysis with aerosol mass spectrometry. Environ. Sci. Technol. 48, 7143–7150. https://doi.org/10.1021/es500486j.

European Environment Agency (EEA), 2025. Air Quality Download Service [WWW Document]. URL https://www.eea.europa.eu/en/datahub/datahubitem-view/778ef9f5-6293-4846-badd-56a29c70880d. (Accessed 4.19.25).

Farr, T.G., Kobrick, M., 2000. Shuttle radar topography mission produces a wealth of data. Eos Trans. Am. Geophys. Union 81, 583–585. https://doi.org/10.1029/EO081i048p00583.

Farr, T.G., Rosen, P.A., Caro, E., Crippen, R., Duren, R., Hensley, S., Kobrick, M., Paller, M., Rodriguez, E., Roth, L., Seal, D., Shaffer, S., Shimada, J., Umland, J., Werner, M., Oskin, M., Burbank, D., Alsdorf, D., 2007. The shuttle radar topography mission. Rev. Geophys. 45. https://doi.org/10.1029/2005RG000183.

Federal Hydrometeorological Institute Bosnia and Herzegovina, 2024. Annual report on air quality in the Federation of Bosnia and Herzegovina for 2023. Sarajevo, BiH.

Federation of Bosnia and Herzegovina, 2024. Law on Air Protection (Zakon o zaštiti zraka). https://fbihvlada.gov.ba/bs/20-zakon-o-zastiti-zraka (Accessed 10.20.25).

Fröhlich, R., Crenn, V., Setyan, A., Belis, C.A., Canonaco, F., Favez, O., Riffault, V., Slowik, J.G., Aas, W., Aijälä, M., Alastuey, A., Artiñano, B., Bonnaire, N., Bozzetti, C., Bressi, M., Carbone, C., Coz, E., Croteau, P.L., Cubison, M.J., Esser-Gietl, J.K., Green, D.C., Gros, V., Heikkinen, L., Herrmann, H., Jayne, J.T., Lunder, C.R., Minguillón, M.C., Močnik, G., O'Dowd, C.D., Ovadnevaite, J., Petralia, E., Poulain, L., Priestman, M., Ripoll, A., Sarda-Estève, R., Wiedensohler, A., Baltensperger, U., Sciare, J., Prévôt, A.S.H., 2015. ACTRIS ACSM intercomparison – Part 2: Intercomparison of ME-2 organic source apportionment results from 15 individual, co-located aerosol mass spectrometers. Atmosph. Meas. Tech. 8, 2555–2576. https://doi.org/10.5194/amt-8-2555-2015.

Fuller, G.W., Tremper, A.H., Baker, T.D., Yttri, K.E., Butterfield, D., 2014. Contribution of wood burning to PM10 in London. Atmos. Environ. 87, 87–94. https://doi.org/10.1016/j.atmosenv.2013.12.037.

Gilman, J.B., Lerner, B.M., Kuster, W.C., Goldan, P.D., Warneke, C., Veres, P.R., Roberts, J.M., de Gouw, J.A., Burling, I.R., Yokelson, R.J., 2015. Biomass burning emissions and potential air quality impacts of volatile organic compounds and other trace gases from fuels common in the US. Atmosph. Chem. Phys. 15, 13915–13938. https://doi.org/10.5194/acp-15-13915-2015.

Grieshop, A.P., Donahue, N.M., Robinson, A.L., 2009. Laboratory investigation of photochemical oxidation of organic aerosol from wood fires 2: analysis of aerosol mass spectrometer data. Atmosph. Chem. Phys. 9, 2227–2240. https://doi.org/10.5194/acp-9-2227-2009.

Grundström, M., Asker, C., Tasse, O., Sievert, U., Gidhagen, L., 2022. Source apportionment with receptor and MATCH modelling in Bosnia and Herzegovina. Report Prepared by the Swedish Meteorological and Hydrological Institute (SMHI).

Hagler, G.S.W., Yelverton, T.L.B., Vedantham, R., Hansen, A.D.A., Turner, J.R., 2011. Post-processing method to reduce noise while preserving high time resolution in aethalometer real-time black carbon data. Aerosol Air Qual. Res. 11, 539–546. https://doi.org/10.4209/aaqr.2011.05.0055.

Henschel, S., Querol, X., Atkinson, R., Pandolfi, M., Zeka, A., Le Tertre, A., Analitis, A., Katsouyanni, K., Chanel, O., Pascal, M., Bouland, C., Haluza, D., Medina, S., Goodman, P.G., 2013. Ambient air SO2 patterns in 6 European cities. Atmos. Environ. 79, 236–247. https://doi.org/10.1016/j.atmosenv.2013.06.008.

Heringa, M.F., DeCarlo, P.F., Chirico, R., Tritscher, T., Dommen, J., Weingartner, E., Richter, R., Wehrle, G., Prévôt, A.S.H., Baltensperger, U., 2011. Investigations of primary and secondary particulate matter of different wood combustion appliances with a high-resolution time-of-flight aerosol mass spectrometer. Atmosph. Chem. Phys. 11, 5945–5957. https://doi.org/10.5194/acp-11-5945-2011.

Hu, W., Hu, M., Hu, W., Jimenez, J.L., Yuan, B., Chen, W., Wang, M., Wu, Y., Chen, C., Wang, Z., Peng, J., Zeng, L., Shao, M., 2016. Chemical composition, sources, and aging process of submicron aerosols in Beijing: Contrast between summer and winter. J. Geophys. Res. Atmosph. 121, 1955–1977. https://doi.org/10.1002/2015JD024020.

Huang, X.-F., He, L.-Y., Hu, M., Canagaratna, M.R., Sun, Y., Zhang, Q., Zhu, T., Xue, L., Zeng, L.-W., Liu, X.-G., Zhang, Y.-H., Jayne, J.T., Ng, N.L., Worsnop, D.R., 2010. Highly time-resolved chemical characterization of atmospheric submicron particles during 2008 Beijing Olympic Games using an Aerodyne High-Resolution Aerosol Mass Spectrometer. Atmosph. Chem. Phys. 10, 8933–8945. https://doi.org/10.5194/acp-10-8933-2010.

Hundt, P.M., Tuzson, B., Aseev, O., Liu, C., Scheidegger, P., Looser, H., Kapsalidis, F., Shahmohammadi, M., Faist, J., Emmenegger, L., 2018. Multi-species trace gas sensing with dual-wavelength QCLs. Appl. Phys. B 124, 108. https://doi.org/10.1007/s00340-018-6977-y.

Huremović, J., Žero, S., Bubalo, E., Dacić, M., Čeliković, A., Musić, I., Bašić, M., Huseinbašić, N., Džepina, K., Cepić, M., Muratović, N., Pašalić, A., Salihagić, S., Krvavac, Z., Zelić-Hadžiomerović, J., Gojak-Salimović, S., 2020. Analysis of PM10, Pb, Cd, and Ni atmospheric concentrations during domestic heating season in Sarajevo, Bosnia and Herzegovina, from 2010 to 2019. Air Qual. Atmosph. Health 13, 965–976. https://doi.org/10.1007/s11869-020-00852-4.

Ingham, D.B., Wen, X., Dombrowski, N., Foumeny, E.A., 1995. Aspiration efficiency of a thin-walled shallow-tapered sampler rear-facing the wind. J. Aerosol Sci. 26, 933–944. https://doi.org/10.1016/0021-8502(95)00028-B.

Institute for Health Metrics and Evaluation (IHME), 2024. GBD 2021 Cause and Risk Summary: Ambient particulate matter pollution. University of Washington, Seattle, WA, IHME.

Institute for Health Metrics and evaluation (IHME), 2024b. GBD Results. IHME, University of Washington, Seattle, WA. Available from: https://vizhub.healthdata.org/gbd-results/. (Accessed 6.12.2025).

Jimenez, J.L., Canagaratna, M.R., Donahue, N.M., Prevot, A.S.H., Zhang, Q., Kroll, J.H., DeCarlo, P.F., Allan, J.D., Coe, H., Ng, N.L., Aiken, A.C., Docherty, K.S., Ulbrich, I. M., Grieshop, A.P., Robinson, A.L., Duplissy, J., Smith, J.D., Wilson, K.R., Lanz, V.A., Hueglin, C., Sun, Y.L., Tian, J., Laaksonen, A., Raatikainen, T., Rautiainen, J., Vaattovaara, P., Ehn, M., Kulmala, M., Tomlinson, J.M., Collins, D.R., Cubison, M.J. E., Dunlea, J., Huffman, J.A., Onasch, T.B., Alfarra, M.R., Williams, P.I., Bower, K., Kondo, Y., Schneider, J., Drewnick, F., Borrmann, S., Weimer, S., Demerjian, K., Salcedo, D., Cottrell, L., Griffin, R., Takami, A., Miyoshi, T., Hatakeyama, S., Shimono, A., Sun, J.Y., Zhang, Y.M., Dzepina, K., Kimmel, J.R., Sueper, D., Jayne, J. T., Herndon, S.C., Trimborn, A.M., Williams, L.R., Wood, E.C., Middlebrook, A.M., Kolb, C.E., Baltensperger, U., Worsnop, D.R., 2009. Evolution of Organic Aerosols in the Atmosphere. Science 326, 1525–1529. https://doi.org/10.1126/science.1180353.

Kim, K.-H., Jahan, S.A., Kabir, E., Brown, R.J.C., 2013. A review of airborne polycyclic aromatic hydrocarbons (PAHs) and their human health effects. Environ. Int. 60, 71–80. https://doi.org/10.1016/j.envint.2013.07.019.

Kolb, C.E., Herndon, S.C., McManus, J.B., Shorter, J.H., Zahniser, M.S., Nelson, D.D., Jayne, J.T., Canagaratna, M.R., Worsnop, D.R., 2004. Mobile laboratory with rapid response instruments for real-time measurements of urban and regional trace gas and particulate distributions and emission source characteristics. Environ. Sci. Technol. 38, 5694–5703. https://doi.org/10.1021/es030718p.

Krechmer, J., Lopez-Hilfiker, F., Koss, A., Hutterli, M., Stoermer, C., Deming, B., Kimmel, J., Warneke, C., Holzinger, R., Jayne, J., Worsnop, D., Fuhrer, K., Gonin, M., de Gouw, J., 2018. Evaluation of a New Reagent-Ion Source and focusing Ion–Molecule Reactor for use in Proton-Transfer-Reaction Mass Spectrometry. Anal. Chem. 90, 12011–12018. https://doi.org/10.1021/acs.analchem.8b02641.

Lalchandani, V., Kumar, V., Tobler, A.M., Thamban, N., Mishra, S., Slowik, J.G., Bhattu, D., Rai, P., Satish, R., Ganguly, D., Tiwari, Suresh, Rastogi, N., Tiwari, Shashi, Močnik, G., Prévôt, A.S.H., Tripathi, S.N., 2021. Real-time characterization and source apportionment of fine particulate matter in the Delhi megacity area during late winter. Sci. Total Environ. 770, 145324. https://doi.org/10.1016/j.scitotenv.2021.145324.

Lanz, V.A., Alfarra, M.R., Baltensperger, U., Buchmann, B., Hueglin, C., Szidat, S., Wehrli, M.N., Wacker, L., Weimer, S., Caseiro, A., Puxbaum, H., Prevot, A.S.H., 2008. Source attribution of submicron organic aerosols during wintertime inversions by advanced factor analysis of aerosol mass spectra. Environ. Sci. Technol. 42, 214–220. https://doi.org/10.1021/es0707207.

Lei, R., Wei, Z., Chen, M., Meng, H., Wu, Y., Ge, X., 2023. Aging effects on the toxicity alteration of different types of organic aerosols: a review. Curr. Pollut. Rep. 9, 590–601. https://doi.org/10.1007/s40726-023-00272-9.

Lelieveld, J., Evans, J.S., Fnais, M., Giannadaki, D., Pozzer, A., 2015. The contribution of outdoor air pollution sources to premature mortality on a global scale. Nature 525, 367–371. https://doi.org/10.1038/nature15371.

Mašić, A., Bibić, D., Pikula, B., Džaferović-Mašić, E., Musemić, R., 2019. Experimental study of temperature inversions above urban area using unmanned aerial vehicle. Therm. Sci. 23, 3327–3338. https://doi.org/10.2298/TSCI180227250M.

Middlebrook, A.M., Bahreini, R., Jimenez, J.L., Canagaratna, M.R., 2012. Evaluation of composition-dependent collection efficiencies for the aerodyne aerosol mass spectrometer using field data. Aerosol Sci. Technol. 46, 258–271. https://doi.org/10.1080/02786826.2011.620041.

Mohr, C., DeCarlo, P.F., Heringa, M.F., Chirico, R., Richter, R., Crippa, M., Querol, X., Baltensperger, U., Prévôt, A.S.H., 2015. Spatial variation of aerosol chemical composition and organic components identified by positive matrix factorization in the barcelona region. Environ. Sci. Technol. 49, 10421–10430. https://doi.org/10.1021/acs.est.5b02149.

Mohr, C., DeCarlo, P.F., Heringa, M.F., Chirico, R., Slowik, J.G., Richter, R., Reche, C., Alastuey, A., Querol, X., Seco, R., Peñuelas, J., Jiménez, J.L., Crippa, M., Zimmermann, R., Baltensperger, U., Prévôt, A.S.H., 2012. Identification and quantification of organic aerosol from cooking and other sources in Barcelona using aerosol mass spectrometer data. Atmosph. Chem. Phys. 12, 1649–1665. https://doi.org/10.5194/acp-12-1649-2012.

Mohr, C., Richter, R., DeCarlo, P.F., Prévôt, A.S.H., Baltensperger, U., 2011. Spatial variation of chemical composition and sources of submicron aerosol in Zurich during wintertime using mobile aerosol mass spectrometer data. Atmosph. Chem. Phys. 11, 7465–7482. https://doi.org/10.5194/acp-11-7465-2011.

Morawska, L., Buonanno, G., 2021. The physics of particle formation and deposition during breathing. Nat. Rev. Phys. 3, 300–301. https://doi.org/10.1038/s42254-021-00307-4.

Müller, T., Fiebig, M., 2018. ACTRIS In Situ Aerosol: Guidelines for Manual QC of AE33 absorption photometer data. https://www.actris-ecac.eu/.

NASA Shuttle Radar Topography Mission (SRTM), 2013. Shuttle Radar Topography Mission (SRTM) Global. Distributed by OpenTopography. Doi: 10.5069/G9445JDF.

Ng, N.L., Canagaratna, M.R., Jimenez, J.L., Zhang, Q., Ulbrich, I.M., Worsnop, D.R., 2011a. Real-time methods for estimating organic component mass concentrations from aerosol mass spectrometer data. Environ. Sci. Technol. 45, 910–916. https://doi.org/10.1021/es102951k.

Ng, N.L., Canagaratna, M.R., Zhang, Q., Jimenez, J.L., Tian, J., Ulbrich, I.M., Kroll, J.H., Docherty, K.S., Chhabra, P.S., Bahreini, R., Murphy, S.M., Seinfeld, J.H., Hildebrandt, L., Donahue, N.M., DeCarlo, P.F., Lanz, V.A., Prévôt, A.S.H., Dinar, E., Rudich, Y., Worsnop, D.R., 2010. Organic aerosol components observed in Northern Hemispheric datasets from Aerosol Mass Spectrometry. Atmosph. Chem. Phys. 10, 4625–4641. https://doi.org/10.5194/acp-10-4625-2010.

Ng, N.L., Herndon, S.C., Trimborn, A., Canagaratna, M.R., Croteau, P.L., Onasch, T.B., Sueper, D., Worsnop, D.R., Zhang, Q., Sun, Y.L., Jayne, J.T., 2011b. An Aerosol Chemical Speciation Monitor (ACSM) for routine monitoring of the composition and mass concentrations of ambient aerosol. Aerosol Sci. Technol. 45, 780–794. https://doi.org/10.1080/02786826.2011.560211.

Offer, S., Hartner, E., Di Bucchianico, S., Bisig, C., Bauer, S., Pantzke, J., Zimmermann, E. J., Cao, X., Binder, S., Kuhn, E., Huber, A., Jeong, S., Käfer, U., Martens, P., Mesceriakovas, A., Bendl, J., Brejcha, R., Buchholz, A., Gat, D., Hohaus, T., Rastak, N., Jakobi, G., Kalberer, M., Kanashova, T., Hu, Y., Ogris, C., Marsico, A., Theis, F., Pardo, M., Gröger, T., Oeder, S., Orasche, J., Paul, A., Ziehm, T., Zhang, Z.-H., Adam, T., Sippula, O., Sklorz, M., Schnelle-Kreis, J., Czech, H., Kiendler-Scharr, A., Rudich, Y., Zimmermann, R., 2022. Effect of atmospheric aging on soot particle toxicity in lung cell models at the air–liquid interface: differential toxicological impacts of biogenic and anthropogenic Secondary Organic Aerosols (SOAs). Environ. Health Perspect. 130, 027003. https://doi.org/10.1289/EHP9413.

Paatero, P., 1999. The multilinear engine: a table-driven, least squares program for solving multilinear problems, including the n-way parallel factor analysis model. J. Comput. Graph. Stat. 8, 854–888. https://doi.org/10.2307/1390831.

Paatero, P., 1997. Least squares formulation of robust non-negative factor analysis. Chemom. Intell. Lab. Syst. 37, 23–35. https://doi.org/10.1016/S0169-7439(96)00044-5.

Paatero, P., Eberly, S., Brown, S.G., Norris, G.A., 2014. Methods for estimating uncertainty in factor analytic solutions. Atmosph. Meas. Tech. 7, 781–797. https://doi.org/10.5194/amt-7-781-2014.

Paatero, P., Tapper, U., 1994. Positive matrix factorization: a non-negative factor model with optimal utilization of error estimates of data values. Environmetrics 5, 111–126. https://doi.org/10.1002/env.3170050203.

Paradiž, B., Belis, C.A., Knezević, J., 2017. Ex-ante assessment of air quality in EUSALPS and EUSAIR macro-regions: towards a coordinated science based approach in support of policy development. Publications Office of the European Union. https://data.europa.eu/doi/10.2760/701646.

Park, M., Joo, H.S., Lee, K., Jang, M., Kim, S.D., Kim, I., Borlaza, L.J.S., Lim, H., Shin, H., Chung, K.H., Choi, Y.-H., Park, S.G., Bae, M.-S., Lee, J., Song, H., Park, K., 2018. Differential toxicities of fine particulate matters from various sources. Sci. Rep. 8, 17007. https://doi.org/10.1038/s41598-018-35398-0.

Pehnec, G., Jakovljević, I., Godec, R., Sever Štrukil, Z., Žero, S., Huremović, J., Džepina, K., 2020. Carcinogenic organic content of particulate matter at urban locations with different pollution sources. Sci. Total Environ. 734, 139414. https://doi.org/10.1016/j.scitotenv.2020.139414.

Pope III, C.A., Dockery, D.W., 2006. Health effects of fine particulate air pollution: lines that connect. J. Air Waste Manag. Assoc. 56, 709–742. https://doi.org/10.1080/10473289.2006.10464485.

Sandradewi, J., Prévôt, A.S.H., Szidat, S., Perron, N., Alfarra, M.R., Lanz, V.A., Weingartner, E., Baltensperger, U., 2008. Using aerosol light absorption measurements for the quantitative determination of wood burning and traffic emission contributions to particulate matter. Environ. Sci. Technol. 42, 3316–3323. https://doi.org/10.1021/es702253m.

Savadkoohi, M., Pandolfi, M., Favez, O., Putaud, J.-P., Eleftheriadis, K., Fiebig, M., Hopke, P.K., Laj, P., Wiedensohler, A., Alados-Arboledas, L., Bastian, S., Chazeau, B., María, Á.C., Colombi, C., Costabile, F., Green, D.C., Hueglin, C., Liakakou, E., Luoma, K., Listrani, S., Mihalopoulos, N., Marchand, N., Močnik, G., Niemi, J.V., Ondráček, J., Petit, J.-E., Rattigan, O.V., Reche, C., Timonen, H., Titos, G., Tremper, A.H., Vratolis, S., Vodička, P., Funes, E.Y., Zíková, N., Harrison, R.M., Petäjä, T., Alastuey, A., Querol, X., 2024. Recommendations for reporting equivalent

black carbon (eBC) mass concentrations based on long-term pan-European in-situ observations. Environ. Int. 185, 108553. https://doi.org/10.1016/j.envint.2024.108553.

Targa, J., Colina, M., Banyuls, L., González Ortiz, A., Soares, J., 2024. Status report of air quality in Europe for year 2023, using validated data, (ETC-HE Report 2025/2). European Topic Centre on Human Health and the Environment.

Tobler, A., Bhattu, D., Canonaco, F., Lalchandani, V., Shukla, A., Thamban, N.M., Mishra, S., Srivastava, A.K., Bisht, D.S., Tiwari, S., Singh, S., Močnik, G., Baltensperger, U., Tripathi, S.N., Slowik, J.G., Prévôt, A.S.H., 2020. Chemical characterization of PM2.5 and source apportionment of organic aerosol in New Delhi, India. Sci. Total Environ. 745, 140924. https://doi.org/10.1016/j.scitotenv.2020.140924.

Tobler, A.K., Skiba, A., Canonaco, F., Močnik, G., Rai, P., Chen, G., Bartyzel, J., Zimnoch, M., Styszko, K., Nęcki, J., Furger, M., Różański, K., Baltensperger, U., Slowik, J.G., Prevot, A.S.H., 2021. Characterization of non-refractory (NR) PM_1 and source apportionment of organic aerosol in Kraków, Poland. Atmosph. Chem. Phys. 21, 14893–14906. https://doi.org/10.5194/acp-21-14893-2021.

Tong, Y., Pospisilova, V., Qi, L., Duan, J., Gu, Y., Kumar, V., Rai, P., Stefenelli, G., Wang, L., Wang, Y., Zhong, H., Baltensperger, U., Cao, J., Huang, R.-J., Prévôt, A.S.H., Slowik, J.G., 2021. Quantification of solid fuel combustion and aqueous chemistry contributions to secondary organic aerosol during wintertime haze events in Beijing. Atmosph. Chem. Phys. 21, 9859–9886. https://doi.org/10.5194/acp-21-9859-2021.

Tuet, W.Y., Chen, Y., Xu, L., Fok, S., Gao, D., Weber, R.J., Ng, N.L., 2017. Chemical oxidative potential of secondary organic aerosol (SOA) generated from the photooxidation of biogenic and anthropogenic volatile organic compounds. Atmosph. Chem. Phys. 17, 839–853. https://doi.org/10.5194/acp-17-839-2017.

Uber Technologies, Inc., 2025. H3: Hexagonal Hierarchical Spatial Indexing.

Ulbrich, I.M., Canagaratna, M.R., Zhang, Q., Worsnop, D.R., Jimenez, J.L., 2009. Interpretation of organic components from positive Matrix Factorization of aerosol mass spectrometric data. Atmosph. Chem. Phys. 9, 2891–2918. https://doi.org/10.5194/acp-9-2891-2009.

Wang, Y., Puthussery, J.V., Yu, H., Liu, Y., Salana, S., Verma, V., 2022. Sources of cellular oxidative potential of water-soluble fine ambient particulate matter in the Midwestern United States. J. Hazard. Mater. 425, 127777. https://doi.org/10.1016/j.jhazmat.2021.127777.

Weichenthal, S., Christidis, T., Olaniyan, T., van Donkelaar, A., Martin, R., Tjepkema, M., Burnett, R.T., Brauer, M., 2024. Epidemiological studies likely need to consider PM2.5 composition even if total outdoor PM2.5 mass concentration is the exposure of interest. Environ. Epidemiol. 8, e317.

Wen, X., Ingham, D.B., 1995. Aspiration efficiency of a thin-walled cylindrical probe rear-facing the wind. J. Aerosol Sci. 26, 95–107. https://doi.org/10.1016/0021-8502(94)00092-D.

World Bank, 2019. Air Quality Management in Bosnia and Herzegovina. World Bank, Washington, DC. http://hdl.handle.net/10986/33043. License: CC BY 3.0 IGO.

World Bank, 2024. Functional Review of Air Quality Management in Canton Sarajevo, Bosnia and Herzegovina. © World Bank.

World Health Organization (WHO), 2021. WHO global air quality guidelines: particulate matter (PM2.5 and PM10), ozone, nitrogen dioxide, sulfur dioxide and carbon monoxide. World Health Organization, Geneva. Licence: CC BY–NC–SA 3.0 IGO.

Ye, Q., Gu, P., Li, H.Z., Robinson, E.S., Lipsky, E., Kaltsonoudis, C., Lee, A.K.Y., Apte, J.S., Robinson, A.L., Sullivan, R.C., Presto, A.A., Donahue, N.M., 2018. Spatial variability of sources and mixing state of atmospheric particles in a metropolitan area. Environ. Sci. Technol. 52, 6807–6815. https://doi.org/10.1021/acs.est.8b01011.

Young, D.E., Allan, J.D., Williams, P.I., Green, D.C., Harrison, R.M., Yin, J., Flynn, M.J., Gallagher, M.W., Coe, H., 2015. Investigating a two-component model of solid fuel organic aerosol in London: processes, PM_1 contributions, and seasonality. Atmosph. Chem. Phys. 15, 2429–2443. https://doi.org/10.5194/acp-15-2429-2015.

Yus-Díez, J., Drinovec, L., Alados-Arboledas, L., Titos, G., Bazo, E., Casans, A., Patrón, D., Querol, X., Gonzalez-Romero, A., Perez García-Pando, C., Močnik, G., 2025. Characterization of filter photometer artifacts in soot and dust measurements – laboratory and ambient experiments using a traceably calibrated aerosol absorption reference. Atmosph. Meas. Tech. 18, 3073–3093. https://doi.org/10.5194/amt-18-3073-2025.

Žero, S., Huremović, J., Memić, M., Muhić-Šarac, T., 2017. Determination of total and bioaccessible metals in airborne particulate matter from an urban and a rural area at Sarajevo. Toxicol. Environ. Chem. 99, 641–651. https://doi.org/10.1080/02772248.2016.1207173.

Žero, S., Žužul, S., Huremović, J., Pehnec, G., Bešlić, I., Rinkovec, J., Godec, R., Kittner, N., Pavlović, K., Požar, N., Castillo, J.J., Sanchez, S., Manousakas, M.I., Furger, M., Prevot, A.S.H., Močnik, G., Džepina, K., 2022. New insight into the measurements of particle-bound metals in the urban and remote atmospheres of the sarajevo canton and modeled impacts of particulate air pollution in bosnia and herzegovina. Environ. Sci. Technol. 56, 7052–7062. https://doi.org/10.1021/acs.est.1c07037.

Zhang, Q., Jimenez, J.L., Canagaratna, M.R., Ulbrich, I.M., Ng, N.L., Worsnop, D.R., Sun, Y., 2011. Understanding atmospheric organic aerosols via factor analysis of aerosol mass spectrometry: a review. Anal. Bioanal. Chem. 401, 3045–3067. https://doi.org/10.1007/s00216-011-5355-y.

Zhang, X., Xu, J., Zhao, W., Zhai, L., Kang, S., Wang, J., Ge, X., Zhang, Q., 2022. High-spatial-resolution distributions of aerosol chemical characteristics in urban Lanzhou, western China, during wintertime: Insights from an on-road mobile aerosol mass spectrometry measurement experiment. Sci. Total Environ. 819, 153069. https://doi.org/10.1016/j.scitotenv.2022.153069.